The International Journal of Engineering and Science (IJES)
|| Volume || 13 || Issue || 5 || Pages || PP 356-398 || 2024 ||
ISSN (e): 2319 – 1813 ISSN (p): 2319 – 1805

Cyclic Voltammetry and its Application to Synthesis New Compounds from Coumarin Derivatives

Ahmed D.H. Deeb, Eman A. BAZ
Department of Physical Sciences, Chemistry Division, College of Science, Jazan University, P.O. Box. 114, Jazan 45142, Kingdom of Saudi Arabia

----------ABSTRACT----------
Cyclic voltammetryhas been applied to a wide variety of new problems. Parallel to this growth the theoretical understanding of these various techniques has been developed. The primary event in most cyclic voltammetricexperiments is the oxidation or reduction of a solution chemical species at an electrode. In this study we can show the application of cyclic voltammetry on some coumarin derivatives to produce a new organic compounds in away easy more than traditional methods of synthesis of organic derivatives of coumarin compound.

Keywords
cyclic voltammetry, glassy carbon electrode, coumarin derivative, cyclic voltammograme, oxidation, reduction

Date of Submission: 14-05-2024 Date of acceptance: 29-05-2024

Theory of voltammetry

During the past three decades, there has been rapid growth in the theory and practice of electrochemistry at stationary electrodes **[1]**. New electrodes materials, such as wax-impregnated graphite, pyloric graphite, carbon paste, and Carbon carbide have been developed. Old electrode materials, platinum and gold, for example have also been applied with good success. Nonaqueous solvents **[2-14]**, primarily acetonitrile and dimethylformamide**[15]**, have received extensive study. New techniques such as linear potential sweep voltammetry, cyclic voltammetry and chronoamperometry have been applied to a wide variety of new problems. Parallel to this growth the theoretical understanding of these various techniques has been developed.

Voltammetry at rotating wire electrodes has been used for many years in analytical chemistry, especially for amperometric titrations. Largely as result of the development of the theory of rotating disc electrodes by Levich and his school in the Soviet Union, voltammetry at rotating electrodes can now be applied to the study of electrode processes in a quantitative way. The primary event in most cyclic voltammetricexperiments is the oxidation or reduction of a solution chemical species at an electrode.

The Fermi level and the Reduction Potential

Consider what happens when an electrode is placed in contact with a solution containing the oxidized and reduced species of a redox couple. Before immersion into the solution, electron in the electrode occupy continuous rang of free energies, according to the conduction band mode (Figure 1). The electron that is easiest to remove is at the top of the conduction band. This energy is termed the Fermi level energy.

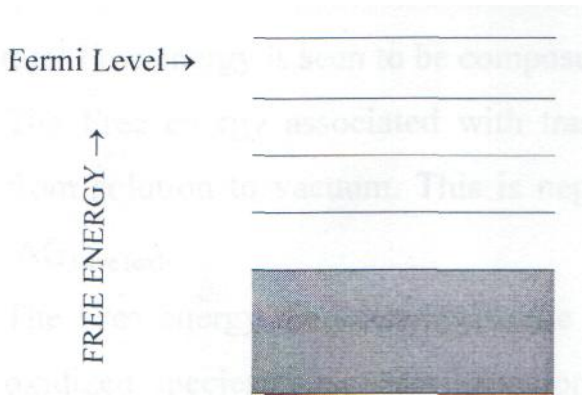

Figure (1) the conduction band model. Conduction is possible when partially filled valance electrodes can be

energy by external fields

The Fermi level is approximately equal (and opposite in sign) to the work function; the amount of energy required to remove an electron from bulk material to vacuum. The free energy change associated with the removal of an electron from the electrode is equal and opposite the Fermi level Free energy. The Fermi level is expressed in units of electron volts (eV); the electron volt is defined as the energy required to move an electron across a potential of one volt. Now let us turn to the process in solution. The Free energy change associated with the transfer of an electron to an oxidized species in solution can be viewed in the context of a thermodynamic cycle.

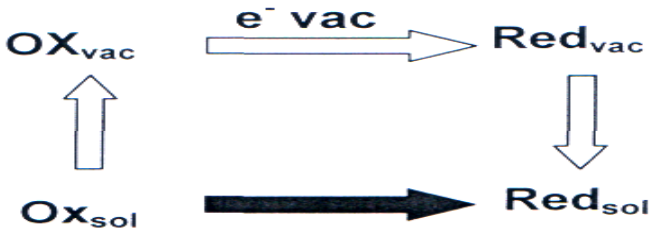

Figure (2) thermodynamic cycle for reduction in solution

The total Free energy is seen to be composed of:

1- The Free energy associated with transfer of the oxidized species from solution to vacuum. This is negative of the solvation energy $-AG_{so}|ve$ (ox)-

2- The Free energy associated with the transfer of an electron to the oxidized species in vacuum (electron attachment) A $G_e i._a t$. This is approximately the electron affinity (EA) of the oxidized species or the negative of the ionization potential (IP) of reduced species.

3- The free energy associated with transfer of the reduced species from vacuum to solution, $AG_{so}i_{ve}$(red)-

$$\Delta G_{abs} = \Delta G_{el.at.} + \Delta G_{solve(red)} - \Delta G_{solve(ox)}$$

The subscript abs denotes that the reference level for energy is established by the electron in vacuo (the absolute scale). If the oxidized and reduced species are at unit activity (at T = 298.15 K°) then the free energy of reduction is a standard free energy and has the usual relationship to the standard reduction potential (also referred to absolute scale), $AG_{abs} = -nFE_{abs}$.

The existence of the oxidized and reduced forms of a redox couple thus determine a kind of Fermi level in solution **[16]**. The Nernst equation for the half-reaction, referenced to vacuum, is then given by:

$$E_{abs} = E^{\circ}_{abs} - \frac{RT}{nF} \ln \frac{[Red]}{[Ox]}$$

A le chatelier "concentration" effect raises or lowers the Free energy of the electrode by the relative concentrations of the reduced and oxidized forms. When an electrode is placed in a solution containing the oxidized and reduced species, the Fermi levels tend to equalize. This is achieved through electron transfer between the electrode and either of the redox species.

Electron transfer from the reduced species to the electrode will raise the Fermi level of the electrode and lower that of the solution. Electron transfer from the electrode to the oxidized species will lower the Fermi level of electrode and raise that of the solution. The total Fermi level energy is usually separated into a chemical part (the innate Fermi level of the metal) and an electrical part (energy as a result of charging) thus we can write.

$$FL_{total} = FL_{innate} - F\emptyset$$

Where *§* is the electrical potential of the electrode. At equilibrium, the total Free energy change must be zero for electron transfer. The Fermi levels are equal. In general both Fermi levels might be expected to move reach equilibrium. In practice however, the electrode potential can be controlled (as in CV experiment) and the solution must adjust. Alternatively, if the electrode potential is not controlled, the solution species can determine the electrode Fermi lever. It is useful to emphasize the distinction between the electrical potential (j) and the Fermi level or the electrode potential E. The electrode potential consists of both the chemical and electrical energy associated with bringing an electron to the electrode, whereas the electrical potential is that part of the energy due to salely to electrostatic effects.

2.2.2 Electrode Kinetics

Electron transfer reactions at the electrode may not be rapid enough to maintain equilibrium concentrations of redox couple species near the electrode surface. The rate equation for heterogeneous electron transfer expresses

the flux of electrons at the electrode surface.

Where A is the area of the electrode (cm), the heterogeneous rate constant is expressed in cm / sec and concentrations are given in moles/ml.

The Hydrogen Reference and Absolute Potential

The preceding discussion used the vacuum level as the reference, to emphasize the relationship between gas phase properties such as IP and EA. Electrochemical measurements however, must utilize a solution based reference. The primary reference is based on the hydrogen ion reduction in aqueous solution:

$$\mathbf{H^+ (aq.unit\ activity) + e^- \leftrightarrow {}^1/_2 H_{2(g,1\ atm)}\ E^O = 0\ volts}$$

For which the potential is taken as E° = 0 volts. The potential for any other half-reaction can in theory be obtained by constructing a complete cell with the hydrogen reaction as anodic (oxidation) and other half-reaction as the cathodic (reduction) reaction figure (2.2). All redox reactions are thus described by their tendency to undergo reduction relative to the hydrogen ion. For instance, the standard potential for the reduction of $Fe(CN)_6^{3-}$ to $Fe(CN)_6^{4-}$ is E° = 0.356, and the reaction

$$\mathbf{Fe(CN)^{3-}_{6(aq)} + H_{2\,(g)} \leftrightarrow Fe(CN)^{4-}_{6(aq)} + 2H^+_{(aq)}}$$

is favorable.

$$\mathbf{(FL_2 - F\emptyset_2) - (FL_1 - F\emptyset_1) = (FL, Cu_2 - F\emptyset_2) - (FL, Cu_1 - F\emptyset_1) = \emptyset_1 - \emptyset_2}$$

What is the relationship between the vacuum (or absolute) potential reference and a reference based on the hydrogen ion reduction? This is the tendency (i.e., the free energy change) for an electron to move from vacuum to reduce the hydrogen ion in aqueous solution.

This quantity is very important in relating electrochemical measurements and gas phase measurements or spectroscopic measurements, and it has been measured to be about 4.42 V however, values around 4.8 V have also been reported **[2, 17 and 18]**. Some physical insight into the origin of the absolute potential is obtained with a thermochemical cycle for hydrogen reduction

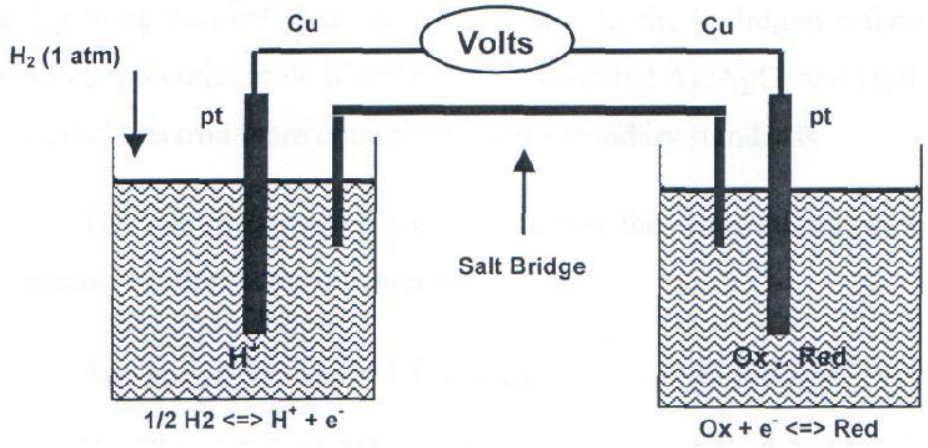

Figure (3) Hypothetical determination of E. Note that a difference in electrode potentials is determined. Since the Fermi levels (FL) of the metals in contact must

equilibrate, the difference in electrode potentials is transmitted exactly a difference in lead electrical potentials, if the leads are of the same material

The individual steps are:

1. Desolvation of H^+.
2. Electron attachment in vacuo to give the hydrogen atom.
3. Formation of molecular hydrogen in the standard state.

The system of standard reduction potentials is described with respect to aqueous solution. Much electrochemical work involves nonaqueous solution, and special consideration must be given to measurements non aqueous media [2]. In cyclic voltammetric studies, it is common to report the reduction potential of a chosen standard, such as the ferrocinium ion under the conditions of the experiment.
The reduction potential of such a large ion is not expected to change appreciably with solvent.

Practical Reference Half-Cells
In practice, electrode reactions other than hydrogen ion reduction are used to construct practical reference systems. Potentials determined using these half-cells can be related back to the hydrogen reference or absolute potential scale if desired. The saturated Ag/AgCl and Hg/Hg_2Cl_2(calomel electrode) are commonly used secondary standards.
The use of saturated solutions keeps the chloride concentrations constant and thus fixes the potential.

$$\mathbf{AgCl_{(s)} + e^- \leftrightarrow Ag_{(s)} + Cl^-_{(aq,sat.kcl)} \quad E^o = 0.199\ V}$$

$$\mathbf{HgCl_{2\,(s)} + 2e^- \leftrightarrow 2Hg_{(L)} + 2\,Cl^-_{(aq,sat.kcl)} \quad E^o = 0.244\ V}$$

The potential of a complete cell is the difference in potential between the cathodic and anodic cell half-reactions:

$$\mathbf{E_{cell} = E_c - E_a}$$

$$\mathbf{E_c = E^o{}_c - \frac{RT}{nF} \ln \frac{[Red]}{[ox]}}$$

$$\mathbf{E_a = E^o{}_a - \frac{RT}{nF} \ln \frac{[Red]}{[ox]}}$$

Where the concentration ratios indicate general reaction quotient terms. The relationship between the concentration and the potential is given by the Nernst equation for the compete cell:

$$\mathbf{E = E^o - \frac{RT}{nF} \ln [Q]}$$

Where Q is the reaction quotient

$$\mathbf{aA + bB \leftrightarrow cC + dD}$$

$$\mathbf{Q = \frac{[C]^c [D]^d}{[A]^a [B]^b}}$$

Note that for a fixed reference system, the cell potential depends on the cathodic reaction components. Again we can note that nonaqueoussystems pose a particular problem

$$\mathbf{E = E^o - \frac{RT}{nF} \ln - 0.199}$$

Note that for a fixed reference system, the cell potential depends on the cathodic reaction components. Again we can note that nonaqueoussystems pose a particular problem.
For instance, if the solvent used in the reference electrode differs greatly from the cell solution, a potential is created (junction potential).

Formal potentials
The E° for a half-reaction is the potential of that reaction versus the standard hydrogen electrode, with all species at unit activity. Most reduction potentials are not determined under such conditions, so it is expedient to define a "formal" reduction potential. This is a reduction potential measured under conditions where the

reaction quotient in the Nernst equation is one and other "non-standard" conditions are described: solvent, electrolyte, pN, and so on. Formal reduction potentials are represented by E°. Reduction potentials determined by cyclic voltammetry are usually formal potentials. The difference between standard and formal potentials is not expected to be great. Other definitions of the formal potential are offered [2].

The Chemical Interpretation of the Reduction Potential [19].

The process of reduction in aqueous solution has been represented by the thermodynamic cycle in figure (2) and the resulting equation:

$$\mathbf{Ox_{(aq)} + e^- \leftrightarrow Red_{(aq)}}$$

$$\mathbf{nFE^o = -\Delta G_{el.\ at.} - \delta\Delta G_{solve} - 4.42\ F + const.}$$

E° is the standard reduction potential based on the hydrogen reference. The hydrogen reduction potentials versus the vacuum is taken as 4.42 V. the constant term accounts for the use of the other references, such as standard calomel electrode (SCE) or the Ag/AgCl electrode (a small contribution to the constant can also come from Junction potentials due to varying solvents, etc). Again, we can note that the free energy of electron association is approximately equal to the electron affinity and to the negative of the ionization potentials.

The Temperature Dependence of the Reduction Potential

The entropy of reduction can be obtained by measuring the reduction potential as a function of temperature:

$$\frac{\delta E^o}{\delta T} = \frac{\Delta S}{nF}$$

In such experiments the temperature dependence of the reference cell potential must be taken into account **[20]**. The most convenient method of doing this entails the use of a "non isothermal" cell. In which the reference is kept at a constant temperature while the temperature of the remaining half-cell reaction is changed.

Transition State Theory for electron transfer

Heterogeneous electron transfer can be envisioned with the aid of transition state diagrams. First consider the forward reaction, the transfer of an electron from the electrode to the oxidized species in solution adjacent to electrode. The reactants are the oxidized species in solution and the electron in the electrode. The free energy of the electron is equivalent to the electrode potential.

Thus the reactant side of the transition state diagram (TSD) reflects the potential of the electrode. The product side of TSD is the free energy of the reduced species in solution. The transition state for electron transfer must depend in some way on physical and chemical changes that occur as a consequence of the electron transfer. The curves in the TSD series figure (4) are related to the free energy relationships that have often been observed by physical organic chemistry for a homologous series of chemical reactions such homologous reaction.

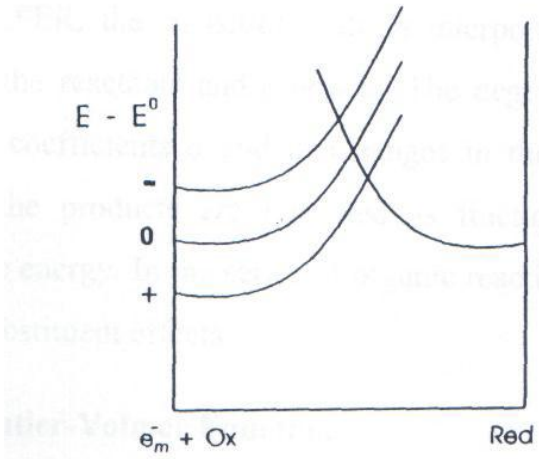

Figure (4) Transition State diagrams for reduction at different electrolyte potentials

Series often follow linear free energy relationships (LFER), where in the following type of relationship

between rate constants and equilibrium constants are observed.

$$\ln [K_f/K_{f(ref)}] = \alpha \ln [K_{eq}/K_{eq(ref)}]$$
$$\ln [K_r/K_{r(ref)}] = \beta \ln [K_{eq}/K_{eq(ref)}]$$

Where the rate and equilibrium constants of a series of homologous reaction are compared to a reference reaction of the series. From the constants $K'_{eq} = l/K_{eq}$ and $Kj/K_r = K_{eq}$ it can be easily shown that B=(l-a). The fundamental equation of transition state theory is:

$$\ln [K] = Z_{exp} [-AG^{++}/RT]$$

Together with the rate/equilibrium relationships this leads to linear free energy relationships for the forward and reverse reactions:

$$A G^{+}_{f} - A G_{ref} = a [AG - A G_{ref}]$$
$$A G_{r} - A G_{ref} = P [AG^{\wedge} - A G_{ref}]$$

In an LFER, the transition state is interpreted as resembling to some degree the reactants and products. The degree of resemblance is given by the coefficients a and p\ Changes in the free energy of the reactants or the products are reelected as fractional changes in the transition state energy. In the series of organic reaction the free energy is changed by substituent effects.

The Butler- Volmer Equation

The free energy of the reactants is changed without any change in the overall reaction (without any chemical change in the reactants or products). It is not surprising that electrochemical kinetics have long been described by an LFER that is called the Butler- Volmer equation. If a reference rates is chosen as the rate when E = E° the forward and reverse rates are equal ($K_f = K_r = K_O$) and we have:

$$A G_{forward} = A G_{ref} + a F [E - E°]$$
$$A G_{reverse} = A G_{ref} + [1- a] F [E - E°]$$

a is referred to as the cathodic or forward transfer coefficient and P=(l- a) as anodic or reverse transfer coefficient form transition state theory the rate is exponentially related to the free energy of activation, so that,

$$\frac{i}{nFA} = K_O \{C_{OX} \exp [-\frac{\alpha nF}{RT}(E - E^O)] - C_{red} \exp[\frac{(1-\alpha)nF}{RT} (E - E^O)]\}$$

=

Which is the Butler- Volmer equation. The standard rate constant KOis a measure of the intrinsic energy barrier. The transfer coefficient a is generally believed to reflect the nature of the transition state **[21-26].**Small values (a > 0.5) are indicative of a product like transition state, and large values (a > 0.5) are indicative of reactant-like transition state.

Marcus Theory [27-29]

The theory that has found the most application for characterizing the nature of outer sphere electron transfers is that developed by R. Marcus, who was awarded of the Nobel Prize in 1992 for these contributions.

The Marcus theory provides a method by which one can relate the rate of electron transfer to salvation reorganization changes structural changes and the overall free energy change. Theory for electron transfer presumes a free equilibrium factor for complex formation and the following electron transfer

$$D + A \leftrightarrow [D, A] \quad K_{eq}$$
$$[D, A] \leftrightarrow [D^{+}, A] \quad K_{et}$$

Kg_t is the rate of electron transfer step.

The Marcusian transfer state diagram presents a reaction coordinate that is composed of solvent reorganization as one move from reactant to product. Transition state diagrams of this sort can be applied to electrode reactions or homogeneous electron transfer figure (2.5).

The free energy along the coordinate varies as a square of the deviation from the equilibrium position. The physical meaning is that small changes in the solvent medium around the ion can give rise to large changes in the electronic energy of the molecule. The intersection of the curves gives the transition state energy. When the driving force AG = 0, the intersection of the two curves occurs at an energy of $A G_0^{++}$ + A-/4. This is called the intrinsic free energy barrier, where A, is related to the optical and static dielectric constants.

$$\lambda = \frac{e^2}{8\pi\varepsilon_0 r} * \left(\frac{1}{\varepsilon_{opt}} - \frac{1}{\varepsilon_{stat}}\right)$$

In polar solvents s_{opt} « E_{stat} and the optical dielectric term dominates. The general expression for the

activation energy is given by:

$$\Delta G^{++} = \Delta G_0{}^{++} * \left(1 + \frac{\Delta G + w}{4\Delta G_O^{++}}\right)^2$$

Where w is the work required to bring the ox and Red to electrode. Often the work term is neglected.

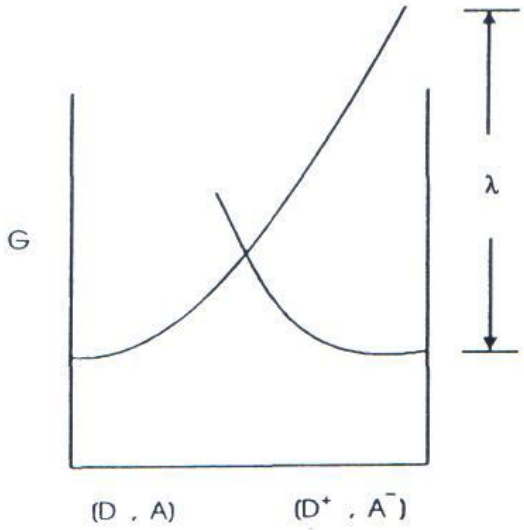

Figure (5) Transition State Diagram for electron transfer according to Marcus Theory**.**

Figure (6) shows the variation of the activation energy with driving force for a typical value of A, 1.00 eV. Inspection of equation (2.17) (after expansion) shows that the free energy relationship, neglecting the quadratic term, is equivalent to the Butler-Volmerequation, with the transfer coefficient set to 0.5. This is shown in figure *1.6)* to be true for small deviations from the reduction potential, for the highly endoergic or exoergic regions, the transfer coefficient (the change in activation energy per change in driving force) is given by:

$$\frac{\partial \Delta G^{++}}{\partial \Delta G^{o}} = \frac{1}{2} + \left(\frac{\Delta G + w}{8\Delta G^{++}}\right)$$

Several cyclic voltammetric studies have shown the expected change in the transfer coefficient with potential **[30]**. The highly exoergic region, where the activation energy increases with driving force, is difficult to observe with electrochemical experiments but has been observed in other contexts **[31].**

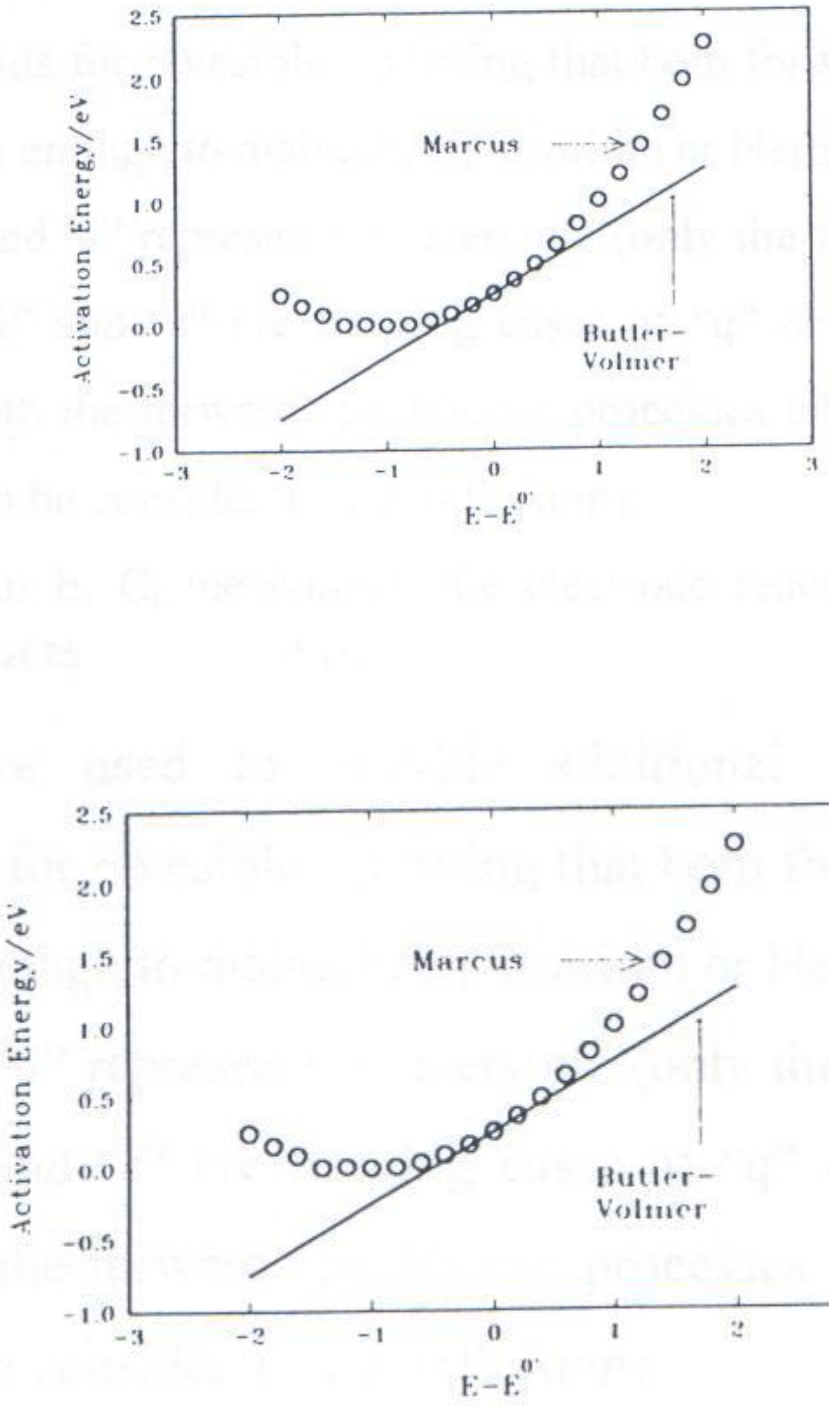

Figure (6) Variation of activation energy with potential according to Marcus theory. The straight line corresponds to a linearized version of Marcus theory, equivalent to theBulter-Volmer equation

The theory is similar for homogeneous electron transfer, except that because there are two ions involved, the value of A is expected to be larger. Also the work terms are different as a result of the difference in work of bringing reactants and products together in solution compared to bringing a single ion to electrode. A term is sometimes included in reorganization energy to accommodate changes in vibrational energies for the molecule / ion transition X =! /2 Zfj 5d; 2 where f is the force constant and 8d is a bond length change. These are sometimes called "inner sphere".

Electrochemical Mechanisms: E & C Notation [32]

The mechanisms are described by E & C notation; E represents a one-electron transfer at the electrode, while C refers to a solution chemical reaction that is coupled to an electrode reaction. For instance, the EC mechanism refers to an electrode reaction followed by a chemical reaction

$$\mathbf{Ox + e^- \leftrightarrow Red}\ \ \mathbf{E^\circ,\ K^\circ,\ a}$$
$$\mathbf{Red \rightarrow products}\ \ K_{dim}$$

Subscripts are used to provide additional information. The subscript "r" stands for reversible (meaning that both forward and reverse processes are fast enough to maintain equilibrium or Nernstain conditions at the surface), and "i" represents irreversible (only the forward reaction is significant); "i" and "r" are limiting cases of "q" or quasi-revesible (meaning that both the forward and reverse processes take place but are not fast enough to be considered at equilibrium).

Thus, in an E_r Q mechanism the electrode reaction is fast and revesible and the chemical reaction is irreversible. Every reductive mechanism has an oxidative analogue. For instance, the oxidative EC is:

$$\mathbf{Red - e^- \leftrightarrow Ox}$$
$$\mathbf{Ox \rightarrow Products}$$

Thus, all the theoretical results quoted for a reductive mechanism can be immediately applied to the analogous oxidative process. The only difference is in the sign of the current and the direction of the potential sweep.

The E_rMechanism

The simplest possible mechanism is the one electron oxidation or reduction of a solution chemical species at the WE. The data can be represented as a current-time curve, or since the potential is linearly related to time for each half-cycle as a current-potential curve are shown in the figure (7). Note that reduction current is taken as positive, the cathodic sweep goes from left to right. For any CV, the direction of the initial sweep should be indicated or at least apparent (the initial sweep potential is always set, if possible, at a potential where zero faradic current occurs).

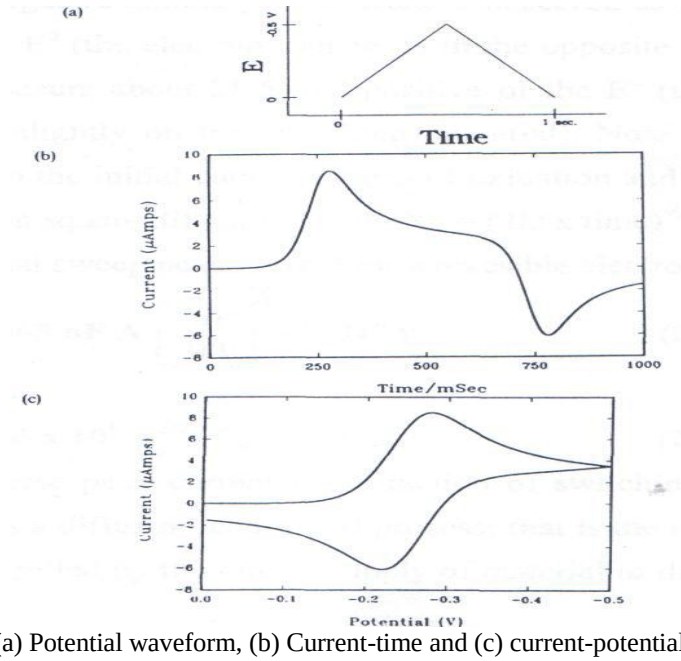

Figure (7) (a) Potential waveform, (b) Current-time and (c) current-potential renresentations

Figure (8), which shows, selected points along the CV with the corresponding concentration profiles of ox and Red. As the potential is swept past the reduction potential, the oxidized form is converted to the reduced form in proportions consistent with the Nernst equation. Because the potential sweep is fast (relative to the rate of diffusion of material to the electrode), the oxidized species is depleted near the electrode. As a consequence of this depletion, cyclic voltammorgams have a peak shape, in contrast to the familiar polarographic sigmoidal wave. Sigmoidal CVs can be indicative of a catalytic regeneration of reactant near the electrode. The peak resulting from the reduction process is called the cathodic peak current, by convention, it is positive, and it is occurs 28.5 mV negative to the E° (at 25°C).

At the switching potential, the direction of the potential sweep is reversed. A negative anodic peak current is observed as the potential is swept past the E° (the electron transfer is in the opposite direction). The anodic peak occurs about 28.5 mV positive of the E° (the exact value depends very slightly on the switching potential). Note that the major perturbation on the initial concentrations of oxidation and Reduction lies within the mean square diffusion length X_D = (2D x time)$^{/2}$.

The initial sweep peak current for a revesible electron transfer is:

$$\mathbf{i_p = 0.4463Nfa}\left(\frac{\mathbf{nF}}{\mathbf{RT}}\right)^{\frac{1}{2}} \boldsymbol{C_{ox}D^{\frac{1}{2}}V^{\frac{1}{2}}} \qquad \textbf{(i)}$$

At 25°C This is: $\mathbf{i_p = 2.686 \times 10^5 n^{\frac{-3}{2}} C_{ox} D^{\frac{1}{2}} V^{\frac{1}{2}} A}$

The reverse peak current is a function of switching potential. A revesible CV is a diffusion-controlled process; that is the rate of electron transfer is controlled by the rate of supply of material to the electrode by diffusion.

Figure (8) the current response and corresponding concentration pro flies (A-F) for a reversible CV. Concentration of the oxidized (solid circle) and reduced form (open circles) are shown as a function of distance from the electrode.

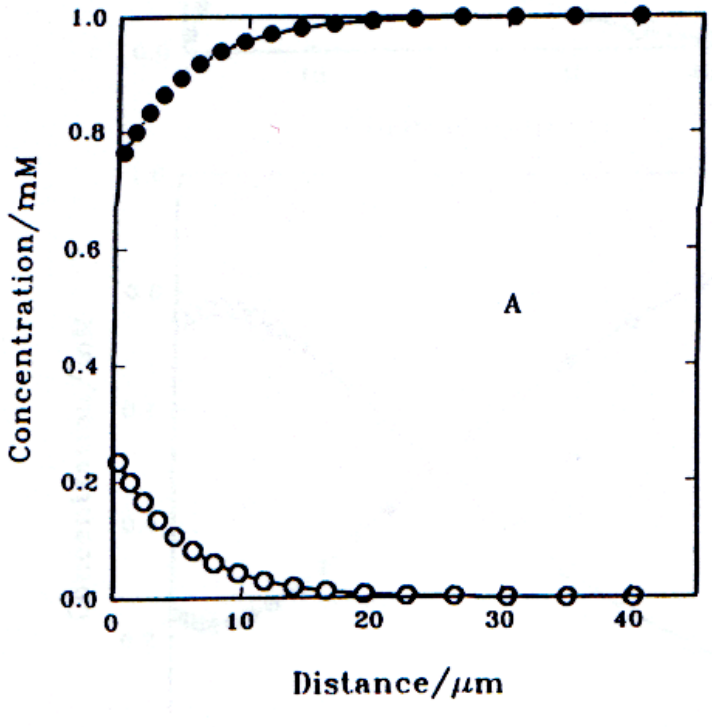

Figure (8) continued

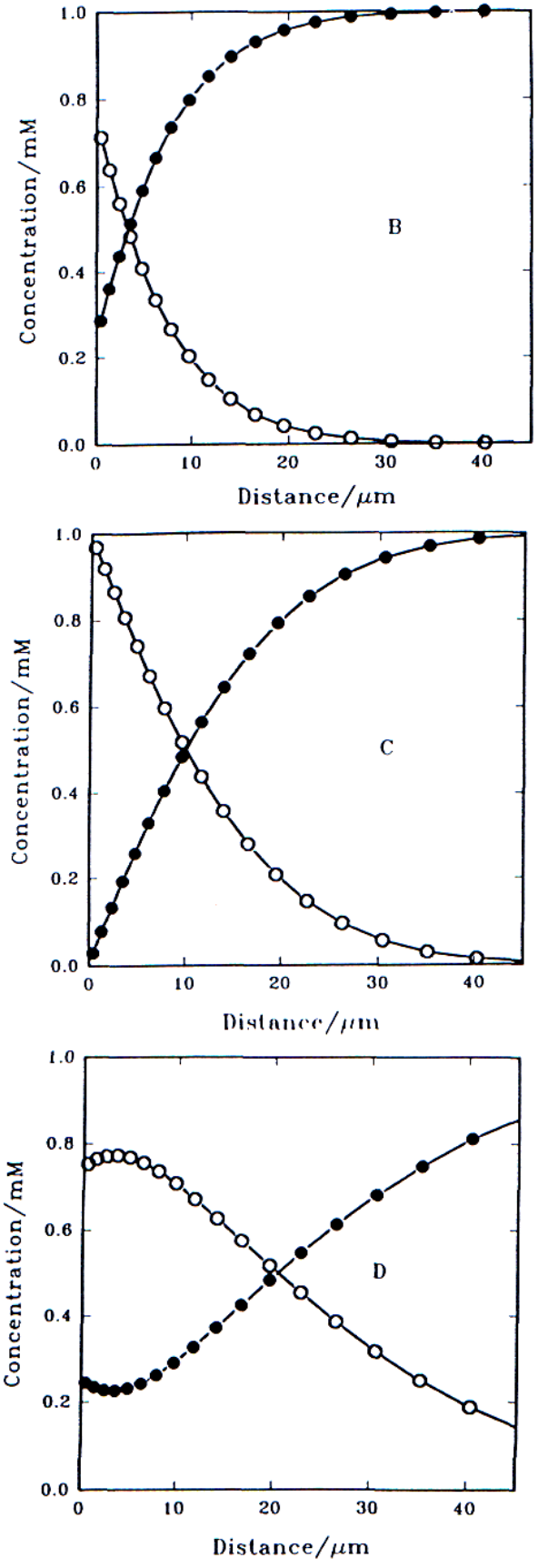

Figure (8) continued

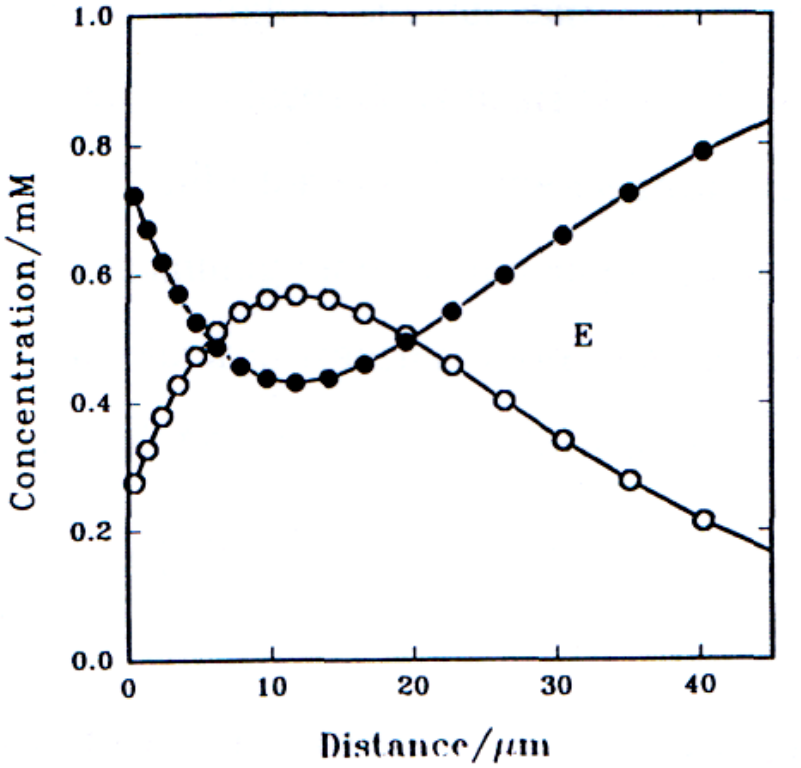
1.0
0.8
0.6
0.4
0.2
0.0
Concentration/mM
E
0
10
20
30
40
Distance/μm

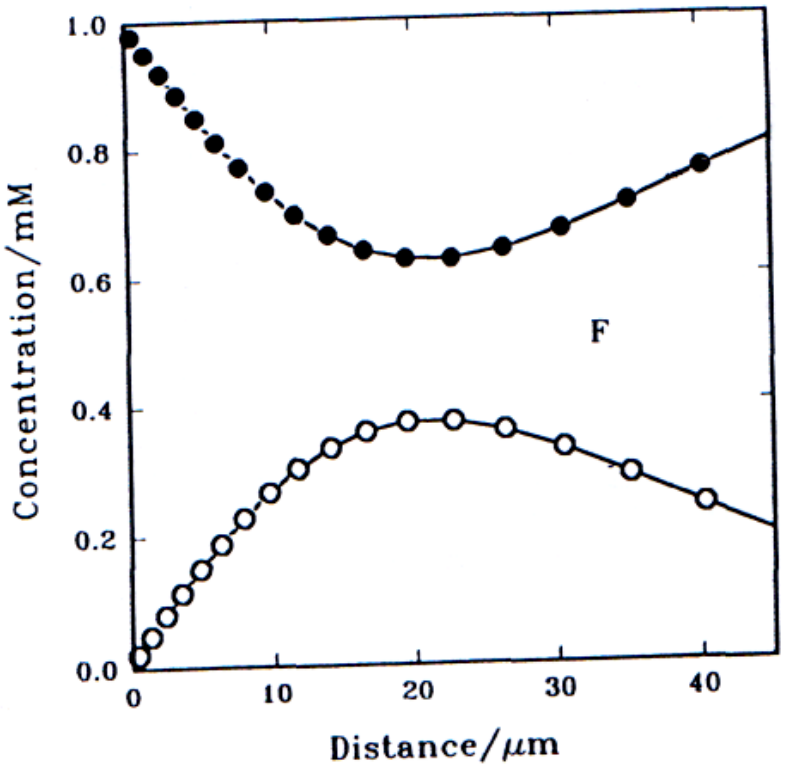
1.0
0.8
0.6
0.4
0.2
0.0
Concentration/mM
F
0
10
20
30
40
Distance/μm

Figure (8)

Multiple sweeps give similar results figure (9) shows a CV with three half-cycles with slightly smaller currents (as the initial condition of (ox) and (Red) near the electrode is nearly but not quite the same for each successive cycle). While for simple one-electron transfer no **information** is to be gained by scanning more than a single cycle, if chemical reactions are coupled to the electron transfer, more than a complete cycle may be informative**.** The peak potential (for the forward seep) is:

$$\mathbf{E_P = E^O - 1.109\left(\frac{RT}{nF}\right)}$$

Assuming that the diffusion coefficients of the oxidized and reduced species are equal. Simulation methods using individual diffusion coefficients give the exact result.

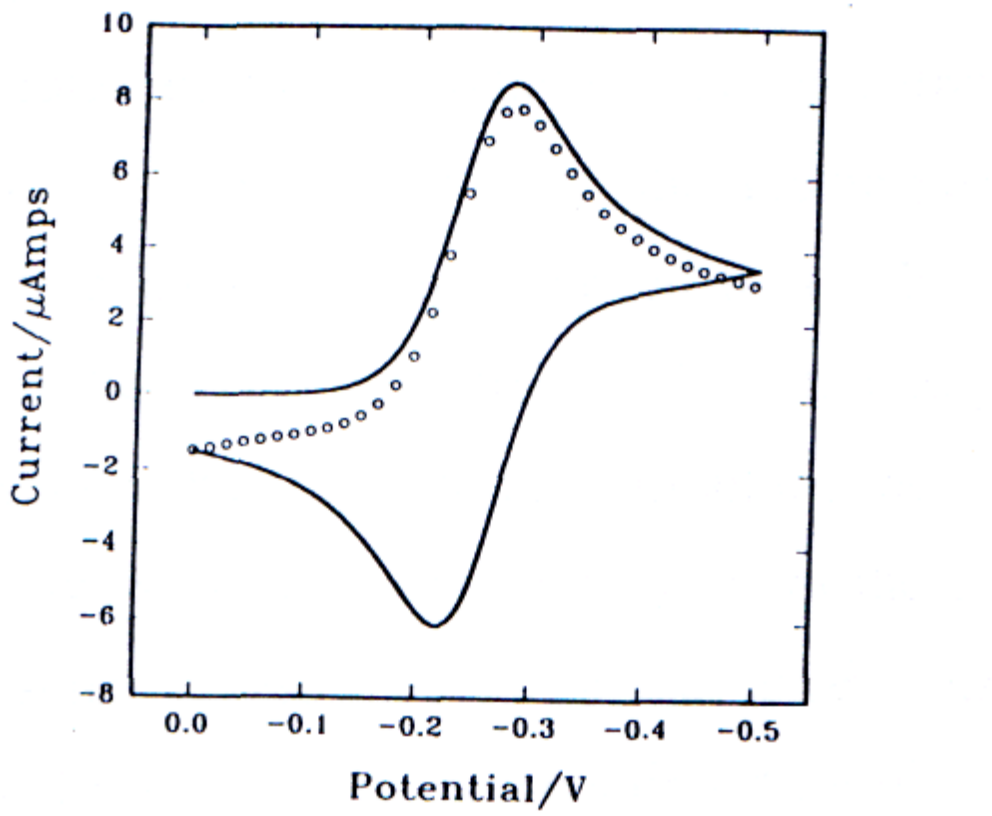

Figure (9) Three half cycles. Note the slight diminution in the second cathodic peak current.

Criterion for the E_r Mechanism

Several criteria can be utilized to confirm a single, revesible, electron transfer.

1- The difference in cathodic (E_{pc}) and anodic (E_{pa}) peak potentials is around 57-60 mV (depending on the switching potential):

$$\mathbf{\Delta E_P = abs\left[E_{p.c} - E_{p.a}\right] \sim 58\ mV}$$

In actual experiments the expected 58 mV is rarely observed because of small distortions due to solution resistance effects and electronic or mathematical "smoothing" of data. The result is that AE_p is often 60-70 mV for revesible electron transfer. For revesiblemultielectron transfer, the peak separation is 60/nmV.

2- The difference between the initial sweep peak and half-peak potentials of the forward sweep is 56 mV/n.

3- The shifted ratio of the cathodic to anodic currents is unity i_{pc}/i^*_{pa}=l **[33].** In the "shifted ratio" the anodic peak current is measured from a baseline that is moved to a value that can be predicted from the decaying portion of the cathodic peak. In this part of the cyclic voltammogram the current can be predicated by assuming an inverse square root dependence of the current of the time. The baseline is assumed to be the current that would be obtained if the forward sweep were continued for the same amount of time that it takes to reach the reverse peak. This procedure is illustrated in figure (10). The absolute ratio (with zero current as a baseline) depends on switching potential **[34-37]**.

4- The forward scan peak current should be proportional to the square root of the scan rate. This criterion is used to distinguish "diffusion-controlled" processes from processes featuring the adsorption of the electroactive species onto the electrode (in which case a linear current - scan rate relationship is observed). A plot of the log i_p versus log v is linear, with a slope of 0.5 for a diffusion peak and a slope of 1 for an adsorption peak intermediate values of the slope are sometimes observed, suggesting a "mixed" diffusion - adsorption peak **[38-41]**.

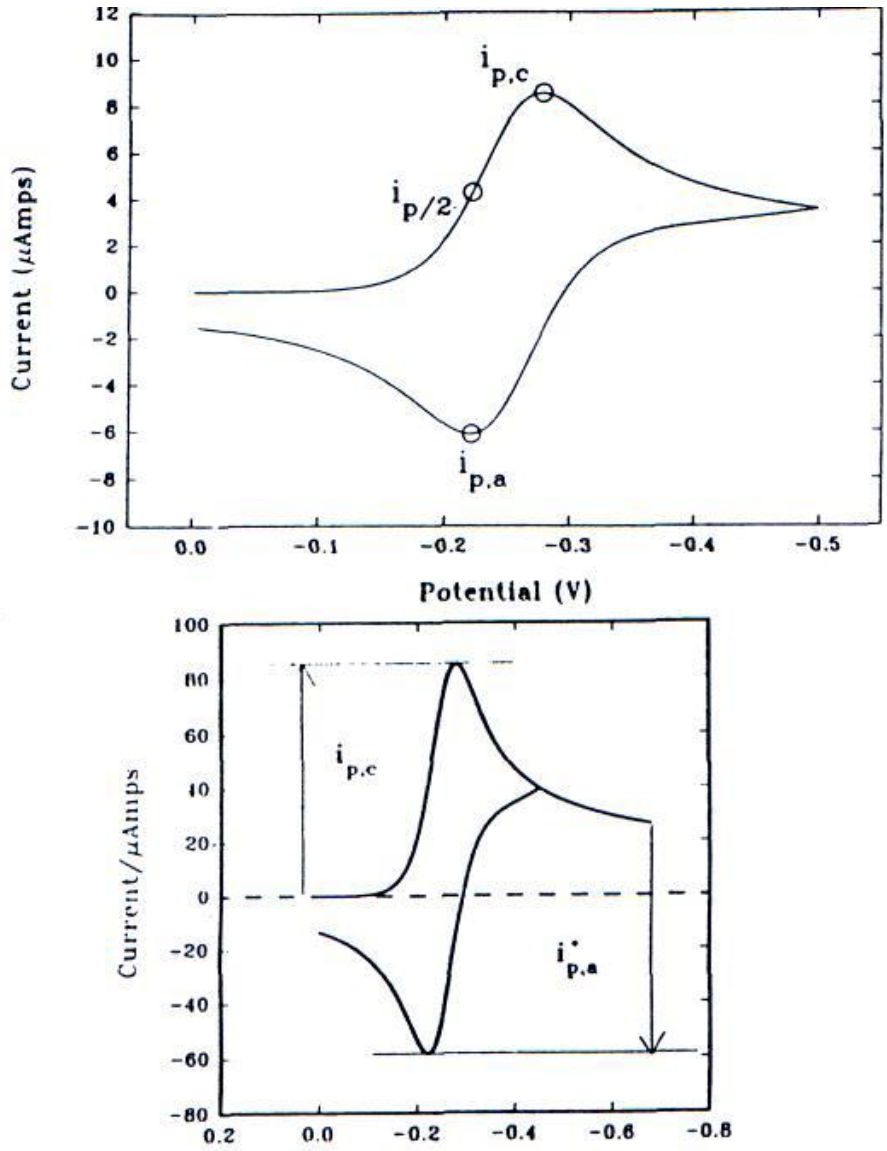

Figure (10) Characteristics of the E_r mechanism: (a) peak potential and current and (b) measurement of the shifted peak current ration.

The Reduction Potential and Number of electrons [42]

1- The reduction potential is given by:

$$E^{O} = \frac{E_{p.c} + E_{p.a}}{2}$$

2- If AE_p has been determined to be 60 mV, and the reduction has been shown to be diffusion controlled, then the number of electrons n = 1, and the diffusion coefficient can be calculated from equation(i).

The geometric electrode area can be found from equation (i) or the effective area can be calibrated with a standard with known D and n. Even if the diffusioncoefficient can be only roughly estimated, a reliable value of n can be found. This is because the current has a square root dependence on D but is proportional to $n^{3/2}$. Conversely, if n is known, the Dox can be determined. The determination of number of electrons involved in an

electrochemical mechanism is crucial but not always as straight forward. This is because the electron transfer is not reversible. The number of electrons can be determined utilizing potential step experiments. Bulk electrolysis (exhaustive electrolysis of all the electroactive species present) is sometimes helpful, but here one must be careful in interpretation because time scales differ widely. Thin-layer bulk electrolysis brings the time scale of the electrolysis more in line with the CV time scale **[38].**

Electrochemical Reversibility

The electrochemical rate equation and its limiting case of very fast rates,
the Nernst equation:

$$\frac{i}{nFA} = K_f C_{ox} - K_r C_{red}$$

$$\frac{K_f}{K_r} = Q = exp\left(\frac{RT}{nF} - (E - E^O\right)$$

If the rate of electron transfer is slow with respect to the time scale of the experiment, then non-nernstian concentrations will exist at the electrode surface. The qualitative effect is to shift the peak wave to more negative potentials in the case of reduction and to more positive potentials in the case of an oxidation. The proximity to equilibrium is termed "reversibility". Increasing the scan rate is equivalent to increasing the rate of diffusion of reduction away from the electrode (for a reductive, ox + e^- = Red, process).At faster scan rates, steeper concentration gradients are produced, increasing the rate of diffusion. Reduction will diffuse away from the electrode faster as the scan rate is increased. The diffusion of Reduction away from the electrode is a process that competes with the oxidation of Reduction. Thus for the E mechanism, the greatest reversibility is observed at slow scan rates. In this case reduction potentials are most accurately measured at slower scan rates, where reversibility is greatest (and distortion least). Three cyclic voltammograms with various degrees of reversibility are shown in figure (11). In the reversible region the CV response is called Nernstianbecause the forward and reverse electron transfers are fast and occur simultaneously. In the irreversible region, the cathodic wave and anodic peaks are well separated, and in each case electron transfer occurs in one direction. The intermediate region is "quasi-reversible". Qualitatively - the demarcation point separating quasi-reversible from irreversible has been reached when there is no (potential) overlap between the cathodic and anodic peak shapes.

The following criteria have been suggested for evaluation of
reversibility, with D = 10^{-5} cm^2/s and T = 298K **[43]**.

Reversible: $K° > 0.3\, v^{1/2}$ cm/s

Quasi-reversible : $K° > 2 \times 10^{-5} v^{1/2}$ cm/s

Totally irreversibl: $K° < 2 \times 10^{-5} v^{1/2}$ cm/s

The experrimenta1ist's attitude toward reversibility or lack of it is shaped by his or her goals. When one desires to obtain information about either reduction potentials or the rates and mechanisms of following chemical reactions, a greater degree of reversibility of electron transfer allows for the use of a wide range of scan rates, and interpretations are simpler. However, studies of the fundamental act of electron transfer are often accomplished with totally irreversible systems. In these cases, the transfer coefficient a and the forward rate of electron transfer are easily measured. The transfer coefficient, being in the exponent of the Butler-Volmerequation**[44]**, and reflecting the symmetry of the barrier to electron transfer, is simply given by:

$$\alpha = \frac{1.857\ RT}{n_a[E_p - E_{P/2}]F}$$

Where $E_{p/2}$ = is the half-peak potential, and n_a is the number of electrons in the rate-determining step. In most circumstances n_a=l. Note that the symmetry of the barrier is reflected in the "steepness" of the cathodic wave figure (12). The anodic transfer coefficient P is determined by the same equation applied to an irreversible anodic wave. For quasi-revesible systems, the reduction potential can be obtained by curve-fitting methods **[45].**If the peaks are symmetrically shaped then:

$$a = 0.5 \text{ and } E^0 \sim [E_{p,c} - E_{p,a}]/2$$

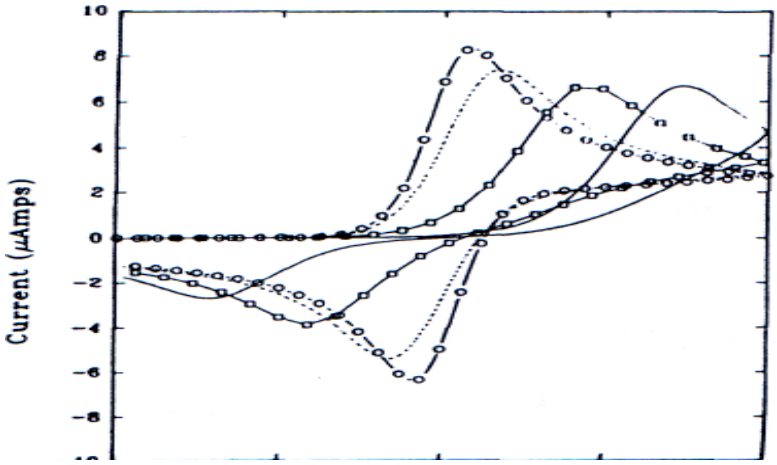

Figure (11) Effect of the heterogeneous rate constants, with the transfer coefficients set to 0.5: circles (reversible), dashed lines (K° = 0.01 cm/s), and solid line (K° = 0.0001 cm/s)

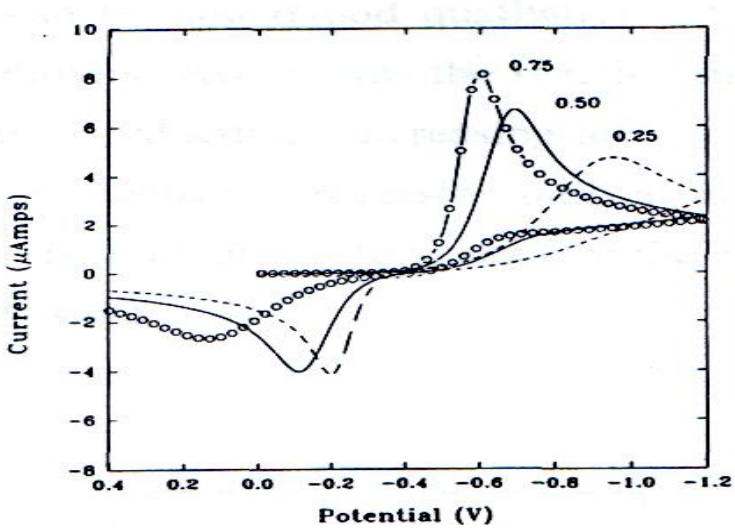

Figure (12) Effect of transfer coefficients for a heterogeneous rage constant K° = 0.0001, with a scan rate of 1 v/s

The EC Mechanism [46]

The EC mechanism recognized by a diminished reverse peak or the lack of one. Both the chemical and electrode reactions may have different degrees of reversibility, which affect the wave shape in characteristic ways. However, at the outset, we will consider the case of a revesibleelectron transfer followed by an irreversible chemical reaction. In this (limiting) case, the CV peak potential will be determined by the E° of the electroactive species and the rate of the following chemical reaction.

The following chemical reaction removes the reduced form solution as it is produced near the electrode. The effect is to shift the peak to more positive values and to increase the peak current slightly figure (13). (At some point, however, the electrode reaction will pushed into the "endergonic" region, and the electron transfer can no longer be considered revesible. Also at potentials negative to E° the backward electron transfer can be small.

This effect can be understood qualitatively on the basis of the Nernst equation (removing Red makes the reaction more favorable and increases the net rate of reduction). Increasing the scan rate has effect of making the CV more chemically reversible until at high scan rates, the chemical reaction is "frozen" on the time scale of the experiment and the CV is completely revesible

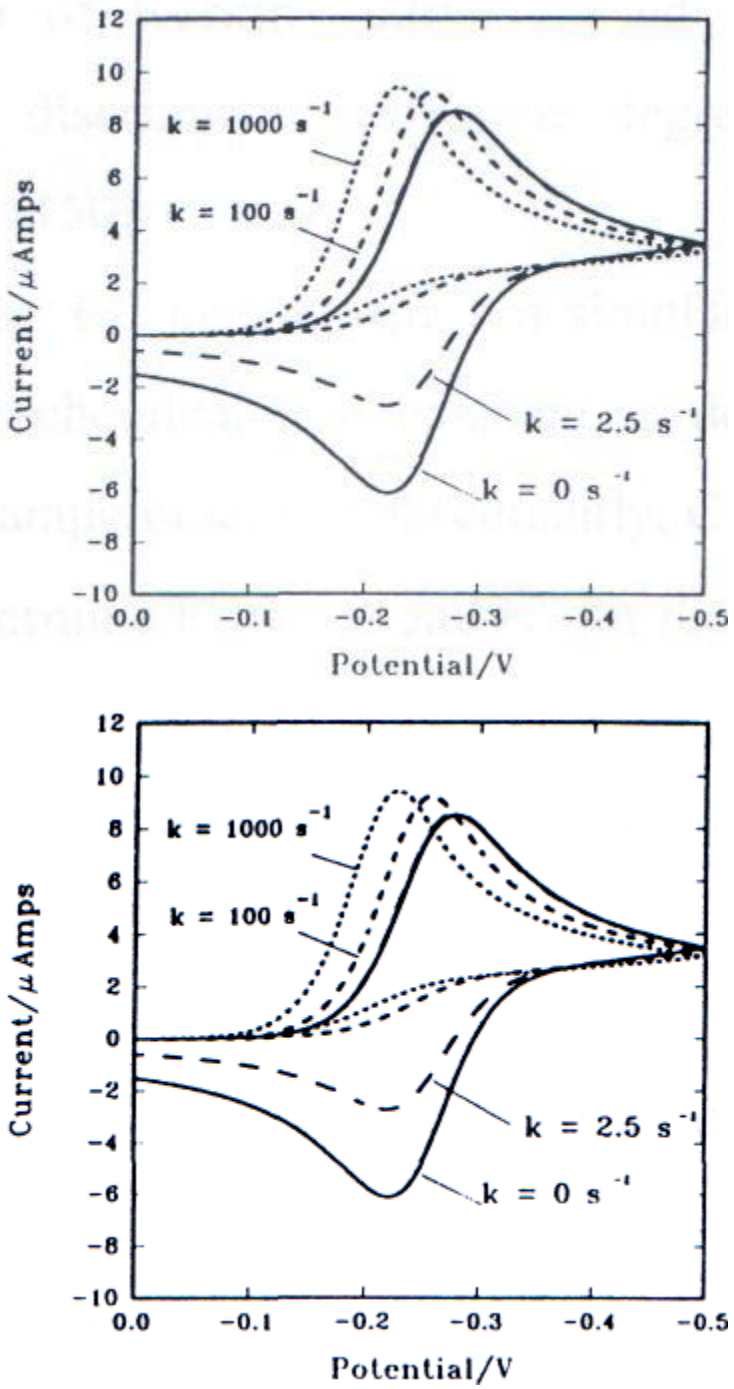

Figure (13) CVs for E_r C, mechanism for a series of increasing solution chemical rate constants at constant scan rate. The same effect would be observed with a constant chemical rate constant and decreasing scan rate

Characteristics of E_r Q Mechanism

1- The ratio of cathodic and anodic peak current is a function of chemical rate constant and scan rate. The cyclic voltammogram can be analyzed to give estimate of the chemical rate constant.

2- The peak potential of the forward scan (when $K_C h_{em}$ RT/nF v >*4)* is given by:

$$E_p = E^O - \frac{RT}{nF}\,0.780 + \frac{RT}{2nF}\ln\left(\frac{K_{Chem}\,RT}{nFv}\right)$$

Several methods have been utilized to determine the rate of the following chemical reaction from a series of CVs at different scan rates. The simplest involves a comparison of $i_{p;C}$ and i^*_{pa} The cathodic peak current is measured from the zero current baseline, while the anodic current baseline is established by the current at which the potential is switched. The experimental peak current ratios can then be compared to a previously calculated theoretical "working" curve to find the rate constant (for a first order or Pseudo-first order reaction) **[47].** Parker has emphasized the use of working curves based on derivative cyclic voltammetry, which discriminates to some degree against capacitive back- ground current **[48]**In analyzing the EC mechanism is a simulation-based method in which the following chemical rate constant is determined by double potential step chronoamperometry. Subsequently, CV simulation analysis can be utilized to determine E° and a and K° for the quasi-revesible case. A simplified two-dimensional "zone" diagram illustrates the situation figure (14). Along one dimension are changes in the heterogeneous rate constant, and along the other dimension are changes in homogeneous rate constant. Cyclic voltammograms for several limiting cases are shown:

1- Irreversible; the electrode kinetics are slow and the chemicalkinetics are slow, the CV is irreversible. The forward peak shifts-59 mV per tenfold change in scan rate.

2- Reversible; The electrode kinetics are fast and the chemicalkinetics are slow, The peak potential is not a function of scan rate,and the CV appears as in the Er mechanism.

3- The electrode kinetics are fast and the chemical kinetics are fast,the peak potential shifts - 30 mV per tenfold change in scan rate.

4- Irreversible. The electrode kinetics are slow and the chemical kinetics are fast. A more detailed analysis can locate intermediate regions.

Reversibility in the zone diagram has an inverse square root dependence on scan rate is equivalent to increasing the rate of diffusion, while in the latter case increasing the scan rate gives less time for the chemical reaction to occur. Thus all else being equal, one can move around in the zone diagram by changing the scan rate. Klinger and Kocki have introduced a quantitative measure of reversibility in electrochemistry as the deviation of the surface concentrations from the values that would exist under Nernstianconditions **[48].** Reversibility thus defined is a function of position along the cyclic voltammogram (i.e. potential). This is because the heterogeneous rates are modulated several orders of magnitude (through the Butler-Volmer equation) over the entire cyclic voltammogram**[47, 49].**

Figure (14) Zone diagram for the EC mechanism,
Typical shapes of voltammograms are given limiting cases.

Scan Rate and the Role of Diffusion [52]

The E_q mechanism the CV wave shape becomes more irreversible with higher scan rates. This happens because increasing the scan rate is equivalent to increasing the rate of diffusion of the oxidized material from the electrode. As a consequence the diffusion process competes with the back electron transfer. The E mechanism can written more generally as follows:

This is shown schematically in figure (15) we have already examined in details the origin of the forward and reverse electron transfer rate constants. In this scheme a diffusion rate constant K_D is introduced. To understand the origin of K_D we take a closer look at diffusion. Cyclic voltammeteric experiments are performed under conditions of so-called semi-infinite linear diffusion. This means that the electrode dimensions are larger than the thickness of the diffusion layer figure (16) and that there is a bulk solution far enough from the electrode that the concentrations of all species remain unchanged throughout the experiment. The symmetry of diffusion under these conditions means that we need consider only diffusion perpendicular to the electrode. No net diffusion takes place in the Y or Z directions, parallel to the electrode surface.

Diffusion is described by Picks' first law of diffusion (equation iii), which states that the number of particles diffusing through a cross-sectional area per unit-time (the Flux J) is proportional to the concentration difference across the selected area. The proportionality constant, which describes the inherent mobility of the particles is calledthe diffusion coefficient (D) and is expressed in square centimeters per second

$$J_i = - D_i \frac{\partial Ci}{\partial x} \qquad \text{(iii)}$$

Taking the derivative of J with respect to distance indicates how the flux changes with distance (the difference between particles coming in the going out) and as a consequence describes the net accumulation of particles at a point (Picks' second law).

Picks' laws follow from the random nature of the motion of particles **[38, 53]**. For linear diffusion the net displacement of particles by diffusion has a square root dependence on time and on the diffusion coefficient. The average net displacement of a particle by diffusion can be shown to be:

$$Ax = (2D\,At)^{r2} \text{(iv)}$$

Equation (iv) can be used to estimate the diffusion layer thickness in a CV experiment.

The diffusion rate is related to scan rate and competes with the reverse rate of electron transfer.

The concentration gradients of the oxidized species (at the cathodicpeak) are shown in figure (17) the surface flux of both species is indicated, and by conservation of material we have:

$$\frac{i}{nFA} = -J_{ox} = J_{red}$$

The irreversible case to make an estimate of the diffusion rate constant K^*_d- The peak current is given by

$$\frac{i}{nFA} = 0.4958\left(\frac{\propto F}{RT}\right)^{1/2} \nu^{1/2} D_{OX}{}^{1/2} C_{OX} = J_{red}$$

The terms multiplying C_{ox} can be taken as the diffusion rate constant, which has the same units as the heterogeneous rate constant K° ($\alpha = 0.5$ and T = 25°C)

$$\mathbf{K_D = 2.18\ (v\ D)}$$

For D = 10"^{5} cm^2/s, we can estimate limiting cases for reversibility, as when one rate constant is two orders of magnitude larger than the order. In this way we arrive at the "quasi-reversible" region ranging from For D = 10"^{5} cm^2/s, we can estimate limiting cases for reversibility, as when one rate constant is two orders of magnitude larger than the order. In this way we arrive at the "quasi-reversible" region ranging from 0.5 $\sqrt{}^2$ (the revesible case) to 5 x 10"^{5} $v^{r/2}$ (the irreversible case).

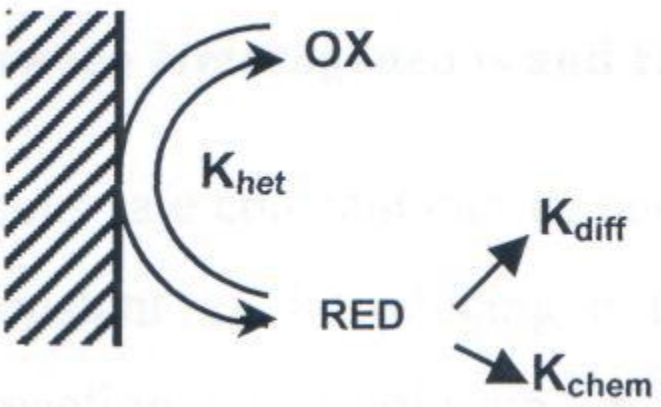

Figure (15) Schematic of the EC mechanism

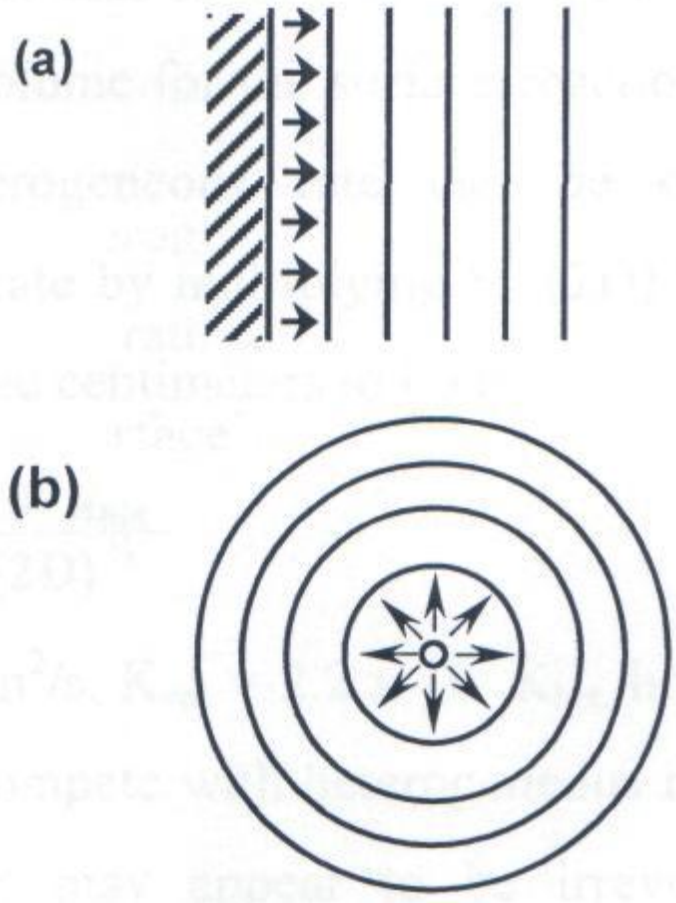

Figure (16) representation of (a) linear and (b) spherical diffusion

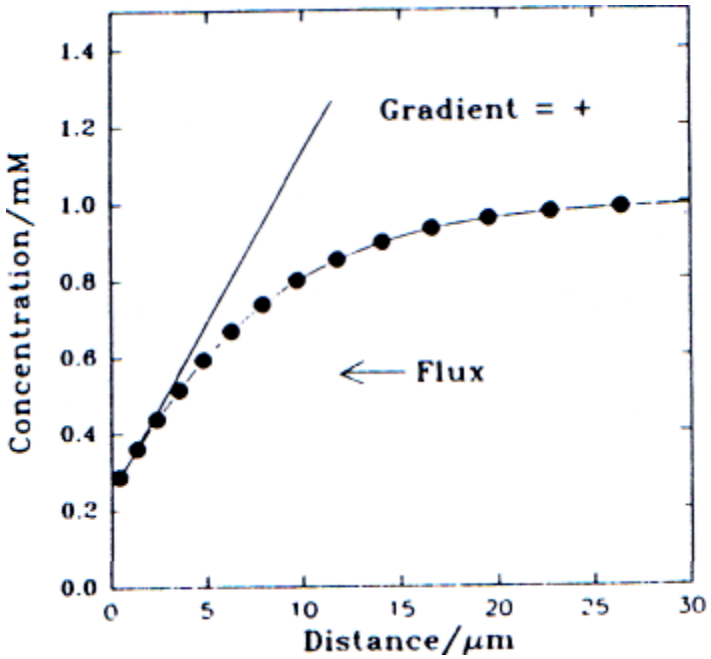

Figure (17) Concentration gradient near the electrode. The tangent at a point determines the direction and rate of diffusion.

Competition between Heterogeneous and Homogenous Reactions

The heterogeneous rate constant can be converted to an equivalent homogeneous rate constant by introducing a third dimension, which coverts the surface reaction rate (mole cm^{-2} s^{-1}) to a volume reaction (mole L^{-1} s^{-1}). A reasonable choice is the diffusion layer thickness at one second (the time unit of the rate constant), shown in figure (18). Thus, the effective volume for the surface reaction is 1cm x 1cm x (2D x ls)$^{1/2}$ cm. The heterogeneous rate can be converted to an equivalent homogeneous rate by multiplying by (2D)$^{-1/2}$. A factor of 1000 takes the result from cubic centimeters to liters.

$$K_{vol} = \frac{10^3 K_{het}}{(2D)}$$

For D = 10^{-5} cm^2/s, K_{VO}| = 2.2 x 10^5K_{he}t. Homogeneous reaction must be rather fast to compete with heterogeneous reactions. Even though cyclic voltammograms may appear to be irreversible (no reverse peak is apparent) the competition between heterogeneous and homogeneous processes makes itself apparent in more subtle ways. The three components of an electrochemical mechanism (disregarding adsorption) are electrode reaction, diffusion and chemical reaction, these rates of this process can be compared in a semiquantitative manner. As a consequence of the effect of scan rate on the CV result for both homogeneous and heterogeneous processes, theoretical presentation often employ dimensionless clusters. For instance, for the E_q mechanism, thefactor:

$$K^O\left(\frac{RT}{nF}\right)^{-1/2}[D\nu]^{-1/2}$$

Controls the result, and for the E_rQ mechanism the controlling factor is:

$$\frac{K_{chem}\,RT}{F\nu}$$

As the mechanisms become more complicated, the number of dimensionless factors needed to characterize the CV response also increases. While this approach is powerful in showing the combined effect of all parameters at once, it can become extremely abstract.

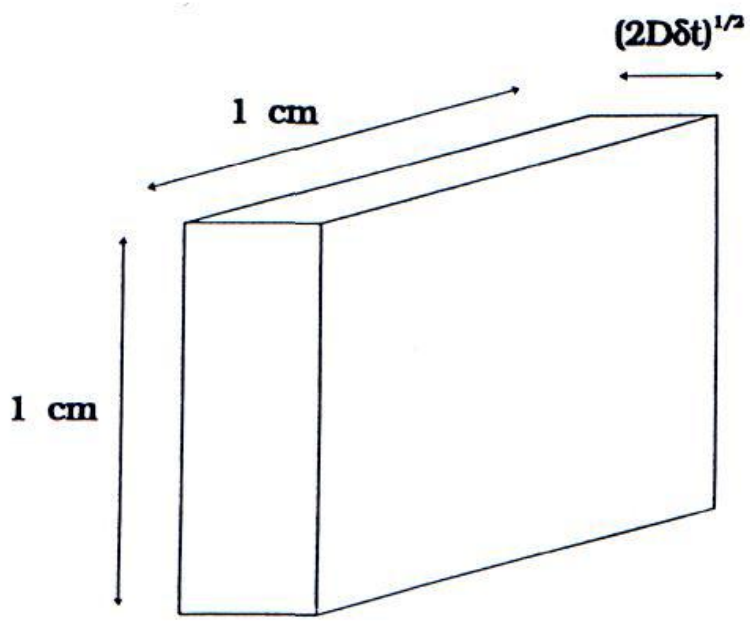

Figure (18) volume of heterogeneous reaction

Distortion of the Faradic Response

There are several experimental realities that tend to distort the observed CV wave shape. Through a combination of experimental and theoretical methods, it is often possible to alleviate these problems to the extent that reliable analyses become possible. An electrical circuit model for the electrochemical cell illustrates the origin of this problem figure (19).

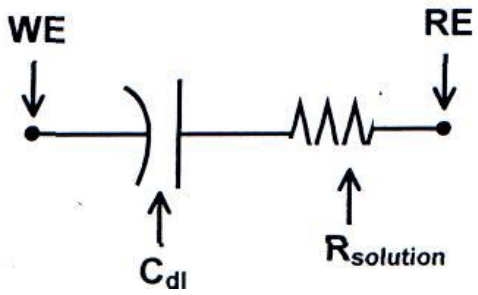

Figure (19) Equivalent circuit for an electrochemical cell

The electrode solution interface is modeled as a capacitor in series with a resistance. The formation of the double layer as potential is changed gives rise to an analogue of an electrical capacitor. So far we have considered in detail only the "ideal" or faradic current due to electrode processes. A complete model of the CV experiment must include the current due to capacitive charging as the potential changes. A resistance element models the resistance between the working electrode and the reference electrode. The potentiostat is controlling and monitoring the potential of the working electrode with respect to reference electrode. To the extent that there is an IR drop across the solution, the potential of the WE will be misrepresented by the monitored potential.

IR Drop

Theoretical treatments of cyclic voltammetry usually assume a cyclic linear potential sweep at the working electrode. However, the solution resistance causes a potential drop to exist across the working electrode and the reference electrode. Thus, the potential at the working electrode is really the applied potential plus the solution IR drop.

$$E_{WE} = E_{APP} + IR_{sol}$$

This equation is sometimes written with R_u to represent "uncompensated" resistance, including the possibility of partial instrumental compensation of the solution resistance. Consider the effect on a typical CV. For positive (cathodic) current, the actual WE potential is less negative than the applied (measured) potential. The effect is to shift peak potentials in a negative direction, For negative (anodic) current, the shift is in the positive direction, Thus, for a reversible electron transfer, AE_P> 58 mV in an experiment that has even a relatively small IR drop. Typical experiment involving 5 uA of current in nonaqueoussolution with resistance of approximately 1000 *Ω.* can result in peak separation about 70 mV. Use of the equation

$$E_{P(corrected)} = E_{P(mean)} + IR_{sol.}$$

is a reasonable way to correct measured peak potentials in solution with moderate resistance problems. Note that the correction for IR drop tracks the current (the anodic and cathodic peak currents differ in sign and in magnitude). The effect of IR drop can be included in simulation treatments. It is best to make reasonable effort to minimize the solution IR drop by:

- Optimizing the electrolyte concentration.
- Placing WE and RE close together
- Using the feedback compensation method, available as an automated option in some commercial units.
- Using smaller electrodes

Capacitive current

Another distortion of the CV from the ideal wave shape arises because the electrode-solution interface acts as a capacitor in series with the solution resistance. The most familiar capacitive current occurs in a potentials step (to a potential at which no faradic current occurs). In this case, the current is given by:

$$I = \frac{\Delta E}{R} e^{-t/RC} \text{dl}$$

Where the total capacitance is:

$$C_{dl} = C/cm^{-2} \text{ x area}$$

Moreover, Δ E is the size of the potential step (V), t is time, and R is resistance. A plot of ln (i) versus time has a slope of - (R Cdi)$^{-1}$ and an intercept ln (ΔE/R). In this way, the capacitance and resistance can be measured figure (20). The C/cm^{-2} (double layer capacitance) for most electrodes falls in the region 10-20 μF/cm^2. For a cyclic linear sweep, the situation is more complex. The double-layer capacitance is in general a function of potential. However, the general features can be described i_th constant capacitance. In this case, the capacitive current rises (starting at Et) with a characteristic time that levels off. Upon the reverse in scan direction, the capacitive current changes sign, the plateau current is equal to the

$i_{cap} = C_d$i x v figure (21), while the faradic current is proportional to the square root of the scan rate. Thus, the distorting effect of capacitive current is largest at higher scan rates figure (22). The ratio of faradic to capacitive current is independent of electrode size.

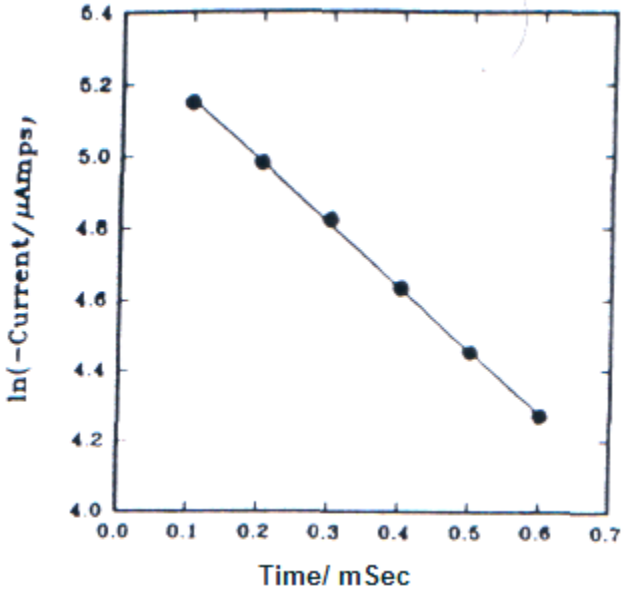

Figure (20) Procedure for measuring resistance and capacitance by a potential step experiment.

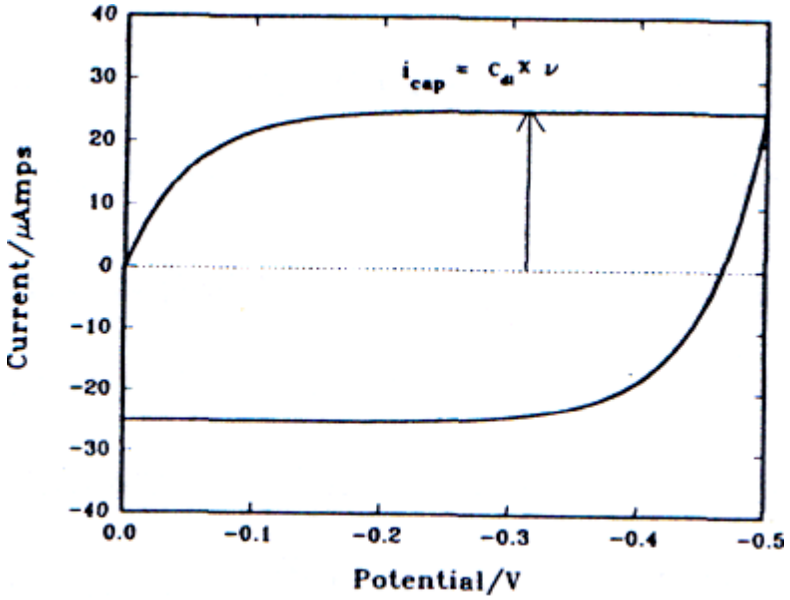

Figure (21) Capacitive response for a cyclic sweep, assuming constant capacitance

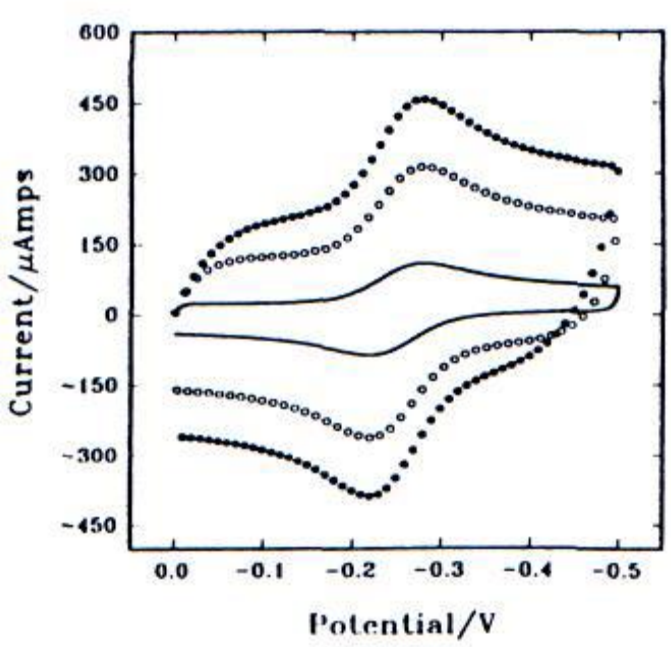

Figure (22) CVs with Capacitive current, assuming typical values for electrode area and capacitance: solid curve, 100; open circle, 500; and solid circles, 850 v/s.

Correcting for capacitive current

There are two approaches to correcting capacitive current: background subtraction an theoretical treatment. In background subtraction, the current obtained from a CV collected in the absence of electroactive species is subtracted from current collected in the presences of electroactive species. This procedure assumes that the double layer remains the same in the two experiments, which is generally true because the double-layer properties are most strongly related to the excess electrolyte. A background subtraction also eliminates the distortion due to residual faradic current from electrolyte and solvent impurities. Theoretical treatment is more difficult since capacitance is a undermined (usually) function of potential. The capacitive current and IR drop are interrelated. Since capacitive current depends on sweep rate, and IR drop causes distortions in linearity of sweep, the capacitance will not follow exactly from theory of linear potential sweep. This effect can be incorporated into finite difference simulations.

Microelectrodes and Fast scan Voltammetry

Electron diameter d is an important experimental variable. For a typical planer disk WE and reference probe, solution resistance is proportional to 1/d, [54]. Whereas the current is proportional to the area or d^2. As a consequence, IR drop is proportional to d. the capacitive rise time decrease as the electrode area is made smaller. (This property is of particular consequence in potential step experiments). With the appearance of microelectrodes and fast potentiostatic circuits the time scale of CV has been extended into submicrosecond range**[55].** As a consequence, faster following chemical reactions can be examined. Note that for fast scan experiments to give useful results, electron transfer must be rather facile figure (23). If the heterogeneous rate constant is too small, the peak currents can be shifted out of the bounds of the potential window at fast scan rates. In using microelectrodes, one must take into account the lower limit of scan rate for which linear diffusion predominates. As the scan rate becomes lower, the predominate mode of diffusion changes over from linear to spherical figure (16). The current response is different for spherical symmetry, because the rate diffusion increases. Microelectrode (slow scan) studies can take advantage of this to measure fast heterogeneous rate constants. The spherical diffusion- limiting current can be compared to the peak current in CV to obtain a lower limit of useful scan rates for studies in the linear diffusion regime. For a one-electron transfer we have:

$$I_{sph} = \frac{2FACD}{d}$$

$$I_p = 0.4463\ FACD^{1/2} \left(\frac{Fv}{RT}\right)^{1/2}$$

The upper and lower scan rate bounds for an electrode of a given diameter for use in the linear diffusion regime based on a 1 or 5% current contribution from spherical diffusion, and a 0.005 or 0.02 V/R drop. As a

consequence of the short time involved in gast scan experiments, total electrolysis is much smaller at microelectrodes, and fouling of electrodes by electrolysis production is minimized.

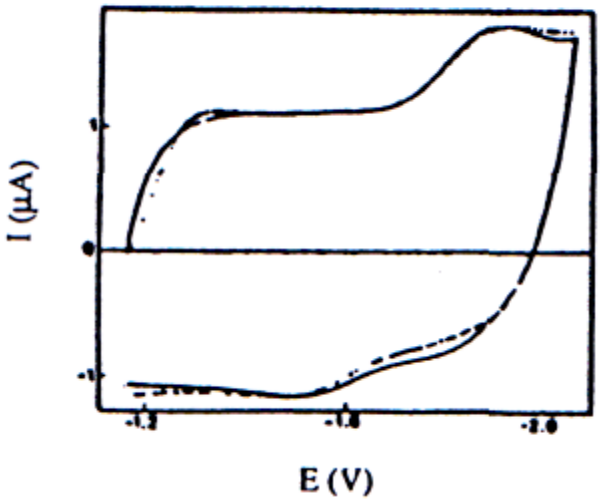

Figure (23) Example of fast scan CV. The reduction of 9- bromoanthracene (10 mM) at a scan rate of 113,000 v/s. (adapted from reference 18).

Electrochemical study of coumarin and coumarin related compounds

Coumarin is widely used as a raw material of blood anti coagulator, **[56, 57]** rodenticide, pesticide**[58-60]**and aromatic essence additive,**[61]** etc., since it has been firstly extracted from Tonka bean. Recently, coumarin derivatives are well known fluorescence dyes for their high photoluminescence (PL) quantum efficiencies, and applied to electro-opticmaterials**[62-65],** reported the results from electro-optic absorption and emission measurements on the equilibrated ground state and the excited Frank-Condon state of four highly efficient coumarin laser dyes Sentient. **[66]**studied the influence of the doping ratio on current-voltage characteristics and electroluminescence quantum efficiency of single layer coumarin doped polymer for blue light-emitting diodes. Justin Tomas **[67]** described the preparation of a coumarin series with peripheral aryl amines, which are green or blue emitting and capable of whole transporting. Chen **[68]** discovered two sterically hindered green coumarin derivatives, which showed significantly thermal stability and overall electrochemical luminescence performance**[69].**

Novel coumarin terminated with poly (p-phenylene) vinylenes were synthesized and the resulting coumarin end capped polymer film gave yellow photoluminescence with a maximum intensity at 560 nm.**[70]**Coumarin modified mesoporous silica expected to open up further application possibilities which can photocontrolled reversible release of guest molecules and drug delivery**.[71]** It was employed as a dye sensitizer **[72]** in dye sensitized solar cells and showed efficient photo-to-electron conversion properties.

On the other hand, electrochemical reduction of coumarin have started to study by Harle**[73]** and Capka**,[74].**Zuman**[75-77]**have reported a half-wave potential and substituents effect for coumarin derivatives and Gourley**[78]**have obtained the result that coumarin derivative becomes dihydrocoumarins by the electrochemical reduction in the presence of tertiary amine coumarin. Reddy**[79]** have suggested a polarographic reaction mechanism of 3-acetyl coumarin and Partridge **[80, 81]**Bond have explained a phenomenon that coumarin becomes adsorbed to mercury electrode. Helin**[82]** have reported the electrochemiluminescence of 4-methyl coumarin derivatives induced by hot electrons into aqueous electrolyte solution. Diez**[83]** have surveyed the voltammetric determination of coumarin in the emulsified media and Wang**[84]**have done a differential pulse voltammetric determination with 7-hydroxy coumarin of human urine. Wang **[85]** have made an amperometric biosensor by modifying antibody of 7-hydroxy coumarin with glassy carbon electrode, and have investigated antibody specificity and antibody-antigen interaction kinetic. 7-hydroxy coumarins were studied using cyclic voltammetry, differential pulse voltammetry, and chronocoulometry. The results showed that the coumarins undergo a pH-dependent, irreversible oxidation with product adsorption**[86].**

In this study, we have performed that the electrochemical reduction and electrogeneratedchemifluorescence of 7-acetoxy-4-bromomethyl-coumarin (ABMC), 7-acetoxymethylcoumarin (AMC), and coumarin as showed the structure in Figure 1 by polarography, cyclic voltammetry (CV), and controlled potential electrolysis (CPE).

Diffusion current of coumarin derivatives.

The typical direct current (DC) and the differential pulse polarograms (DPP) of coumarin, AMC and ABMC in 0.1 M TEAP-AN solution were obtained. The polarograms and cyclic voltammograms are shown in Figure 25, and Figure 26, respectively. We were able to interpret that step 1 was bromide reduction of ABMC and step 2 was reductive hydrogenation **[87,88]** of coumarin ring carbonyl group and step 3 was cleavage of ABMC acetoxy group or dehydrogenation of coumarin ring double bond and dimerization in Figure 25 and Figure 26. In order to know whether each reduction wave is caused by a diffusion wave or by a chemical reaction, it is firstly investigated the changes of the limiting current according to increases in concentration. The reduction waves were proportionated to concentration indicating that the currents was caused by diffusion. As the second proof of diffusion current, **[89]**DC polarogram was obtained and calculated the percentage of $\Delta i/\Delta T$ by changing the temperature condition of a sample solution at intervals of 5 ° C from 10° C to 35 ° C. From the result that $\Delta i/\Delta T$ percentage for reduction stage 1, 2 and 3 are 1.09, 1.26 and 1.05% respectively, we could assure that each reduction current is diffusion current. The diffusion current 35 is proportionate to $m^{2/3} t^{1/6}$ according to Ilkovic equation. DC and DP polarograms were obtained by changing drop's lifetime of mercury into 0.5, 1, 2 and 5 sec, and weighed the dropped mercury drops per lifetime for a fixed time in a blank solution. Reduction current values acquired from each reduction step 1, 2 and 3 have showed a good proportion to $m^{2/3}t^{1/6}$ values of mercury drop. From the result of cyclic voltammogram as shown in Table 2, ipc/ values were nearly constant for the different scan rate. These various results showed that each reduction step of ABMC is diffusion controlled ones.

Figure (24). Structure of A: coumarin, B: 7-acetoxy-4-methyl-coumarin (AMC),
C: 7-acetoxy-4-bromomethyl-coumarin (ABMC).

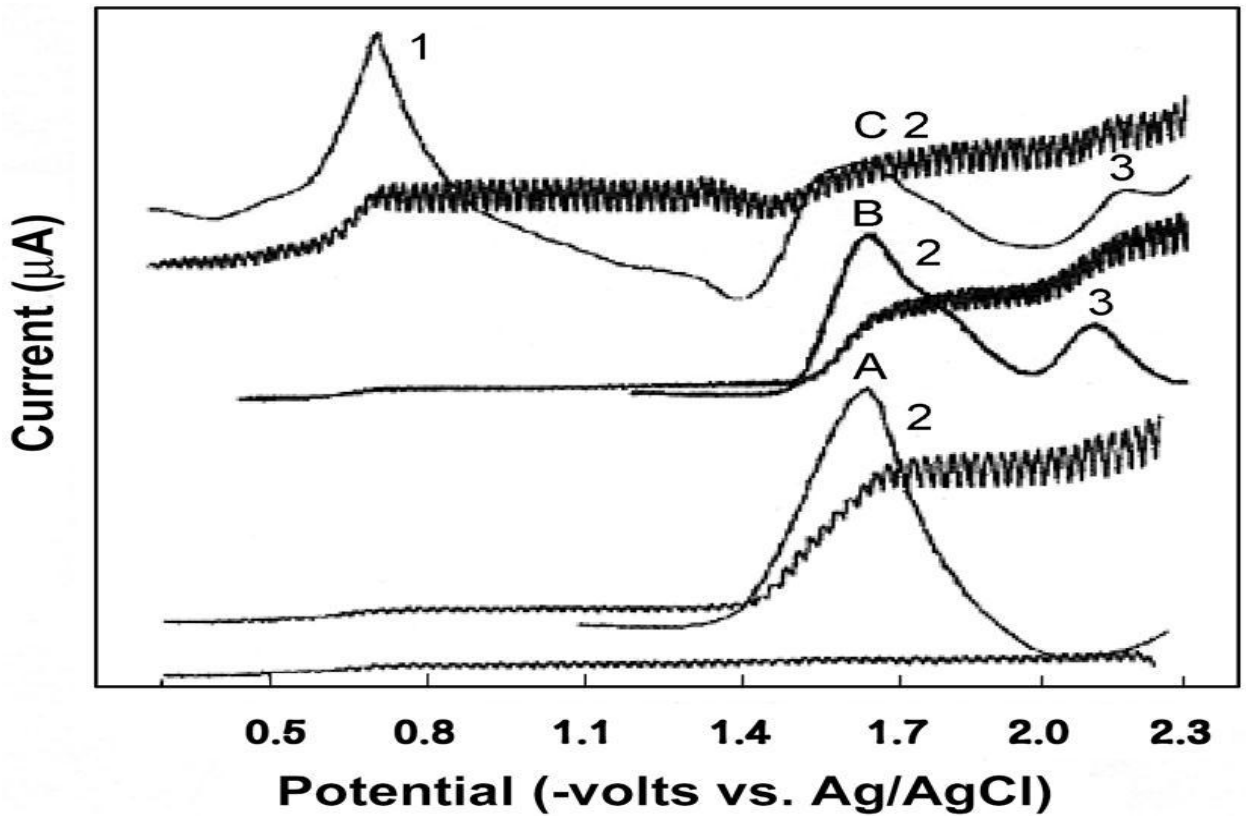

Figure (25). Typical DC and DP polarograms of coumarin derivatives in 0.1 M TEAP-AN solution. Scan rate: 50 mV/sec. Current range: 0.02 mA. A: 1 × 10−3 M coumarin, B: 1 × 10−3 M AMC, C: 5 × 10−4 M ABMC.

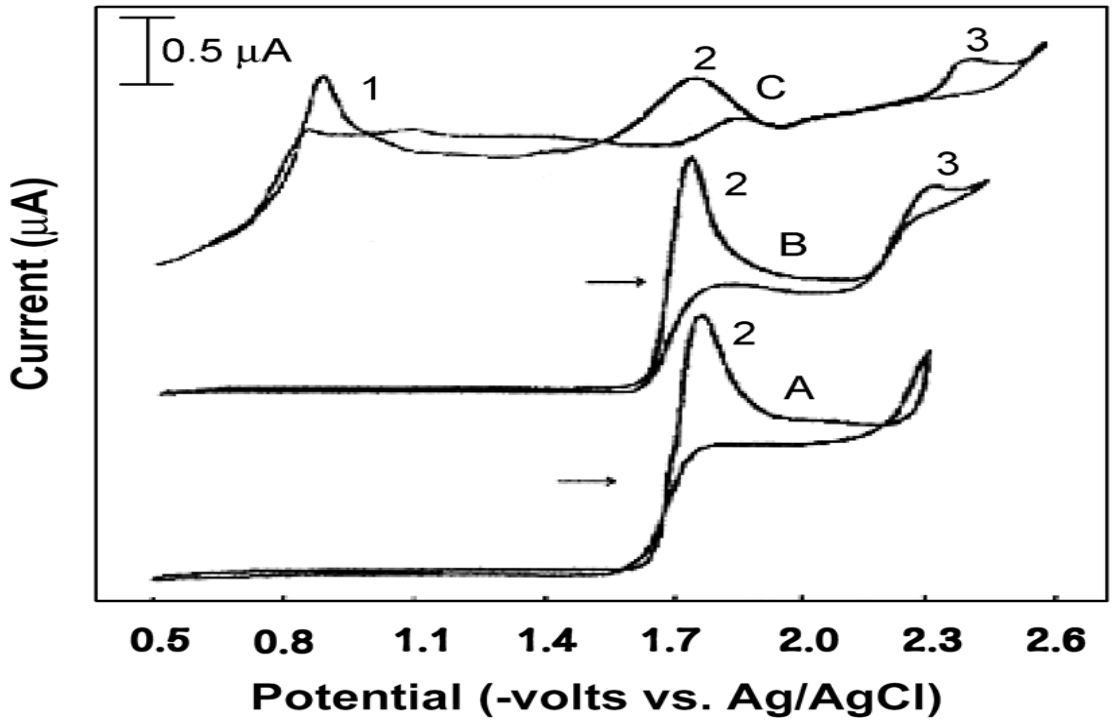

Figure (26). Typical cyclic voltammograms of coumarin derivatives in 0.1 M TEAP-AN solution. Scan rate: 50 mV/sec. A: 1 × 10−3 M coumarin, B: 1 × 10−3 M AMC, C: 5 × 10−4 M ABMC.

Irreversibility of Electrochemical Reduction of Coumarin Derivatives

On the plot of log [i/(id − i)] vs. potentials for polarograms, if the slope value is 59.1/n mV or the potential difference value of $E^{3/4}$-$E^{1/4}$ comes to 56.4/n mV, the electrode reaction is close to reversibility.An irreversible process can defined as the peak potential difference between E_{pc} and E_{pa} becomes larger the above criteria. For a totally irreversible wave, i_p is also proportional to Co * and $\sqrt{v}$, but E_p is a function of scan rate, shifting to a negative potential direction by an amount 30/α na mV for each tenfold increase in scan rate at 25 ° C. When the slope of the 1st reduction wave is 84 mV and $E^{3/4} - E^{1/4}$ value is 82 mV, and the slope of the 2nd reduction wave is 73 mV and $E^{3/4} - E^{1/4}$ value is 72 mV, it means that the 1st and 2nd reduction waves were proceeded to the irreversible process. And, the peak potential has moved to negative potential over 30/α na mV as scan rate increased, which is interpreted as an irreversible process. For the all of the three reduction waves, each anodic peak current for cathodic peak currents did not appear in CV.

The electrochemical reductions of AMC and ABMC were proceeded with the three irreversible steps (−1.2, −1.8, −2.3volts). EC mechanism consisting of the removal of bromo group at first step, and acetoxy group at the third step was proposed. Coumarin derivatives have shown blue colored fluorescence by the controlled potential electrolysis at over −1.8 volts. Fluorescence intensity of coumarin attached with electron releasing group was higher than coumarin basic molecule. The fluorescence intensities of AMC and ABMC were enhanced when controlled potential electrolysis was proceeded at more negative potentials as (−2.3 volts). This electrogenerating technique using CPE to obtain enhanced fluorescence compounds will be useful to development for electro-optic materials or laser dyes **[90]**.

Scheme (1). The proposed electrochemical reduction mechanism on the ABMC.

Cyclic voltammetry of 4-(bromomethyl)-2-oxo-2H-chromen-7-yl acetate.

Curve A in Figure 28 is a cyclic voltammogram recorded at a scan rate of 100 mV s^{-1} for the reduction at a glassy carbon electrode of a 5.0 mM solution of 4-(bromomethyl)-2-oxo-2H-chromen-7-yl acetate in oxygen-free DMF containing 0.10 M $TMABF_4$; this cyclic voltammogram shows four distinct irreversible cathodic peaks with E_{pc} values of -0.16, -0.86, -0.97, and -1.64 V, respectively. We attribute the first cathodic peak to one-electron reductive cleavage of the carbon–bromine bond, as demonstrated later in this report. On the

basis of separate studies, we associate the peaks at -0.97 and -1.64 V with the electrochemical reductions of 2 and 3, respectively, which are products of a bulk electrolysis of 1 at -0.20 V. Curve B in Figure 28is a cyclic voltammogram obtained under the same experimental conditions described above, but it was recorded after an exhaustive controlled-potential (bulk) electrolysis of 1 at -0.20 V. It is readily apparent that the first peak in curve A is no longer present. Note that curve B of Figure 28 shows a new, small cathodic peak at -0.63 V; close inspection of curve A of Figure 28reveals a barely discernible bump (between larger peaks at less and more negative potentials) that seems to correspond to the new peak at- 0.63 V.

A cyclic voltammogram for a 5.0 mM solution of 1 in CH_3CN containing 0.050 M $TMABF_4$ is depicted in curve A of Figure 29; except for a change in the solvent–supporting electrolyte, the experimental conditions were the same as those described in the preceding paragraph. In curve A of Figure 29, there are four cathodic peaks at - 0.084, - 0.70, - 0.97, and -1.14 V that are associated with the reduction of 1. Notice that the first, second, and fourth peak potentials for the CH_3CN–$TMABF_4$ system are more positive than those for the DMF–TMABF4 system, whereas the third peak potential is the same for both media. Curve B in Figure 29 is a cyclic voltammogram obtained after a bulk electrolysis of 1 at - 0.20 V. It is obvious that curve B in Figure 29 (with only a single peak corresponding to reduction of 2 at - 0.97 V) differs considerably from curve B of Figure 28 (which shows four peaks).

To clarify this latter discrepancy between the behaviors in the two different solvent–electrolyte systems, separate cyclic voltammograms for 5.0 mM solutions of 2 and 3 in CH_3CN–0.050M $TMABF_4$ were recorded, as illustrated in curves A and B of Figure 30, respectively. As curve A reveals, the only voltammetric response for either species is a cathodic peak at - 0.97 V for the monomeric product (2). We have found that the insolubility of product species 3 in CH_3CN–$TMABF_4$ (and indeed in most organic solvents) makes cyclic voltammetric experiments impossible. In fact, when we attempted to introduce 3 into CH_3CN–$TMABF_4$, it did not dissolve, and no voltammetric response could be observed (curve B, Figure 30)**[91].**

Figure (27)

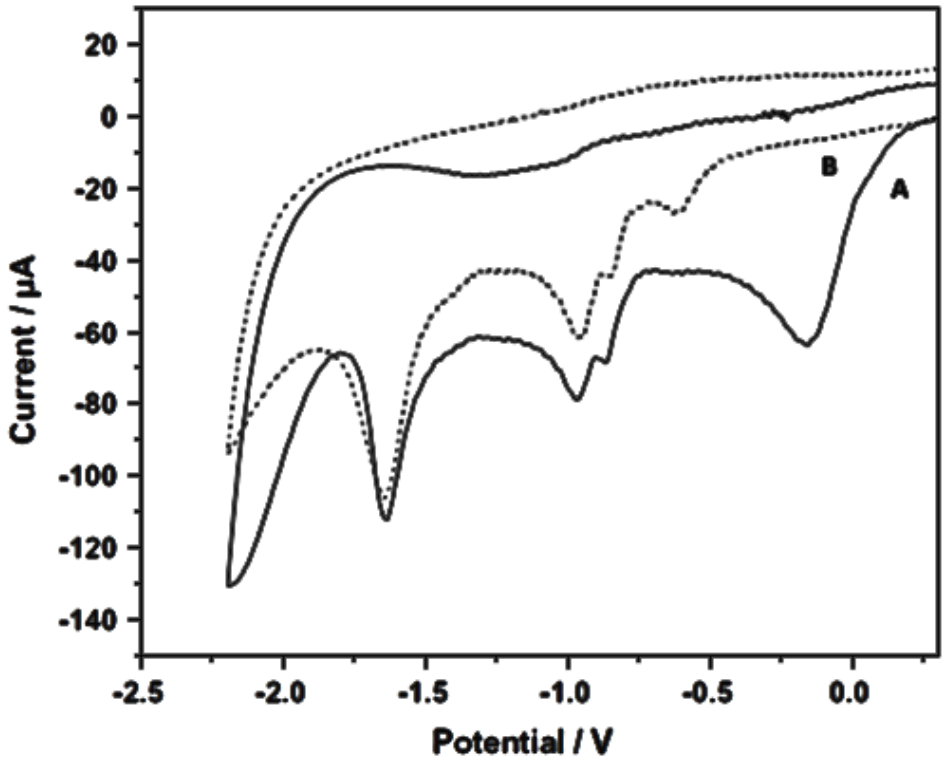

Figure (28). Cyclic voltammograms recorded with a glassy carbon disk electrode (area = 0.077 cm^2) at 100 mV s^{-1} in oxygen-free DMF-0.10 M $TMABF_4$ containing 5.0 mM 4-(bromomethyl)-2-oxo-2H-chromen-7-yl acetate (1) both prior to (A) and immediately after (B) controlled-potential (bulk) electrolysis performed at -0.20 V. Scans go from ca. +0.25 to -2.25 to +0.25 V.

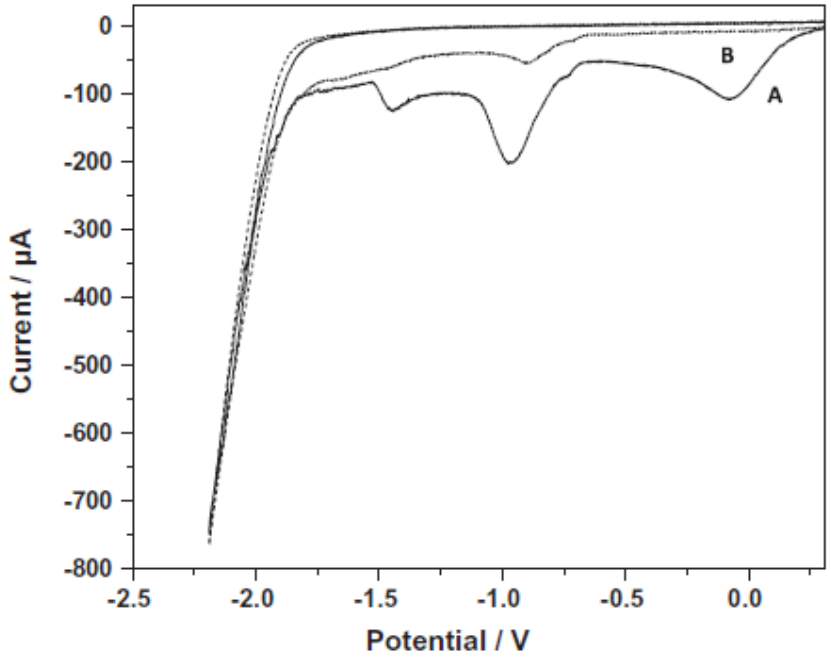

Figure (29). Cyclic voltammograms recorded with a glassy carbon disk electrode (area = 0.077 cm2) at 100 mV s^{-1} in oxygen-free CH_3CN–0.050 M $TMABF_4$ containing 5.0 mM 4-(bromomethyl)-2-oxo-2H-chromen-7-yl acetate (1) both prior to (A) and immediately after (B) controlled-potential (bulk) electrolysis performed at -0.20 V. Scans go from ca. + 0.25 to - 2.25 to + 0.25 V.

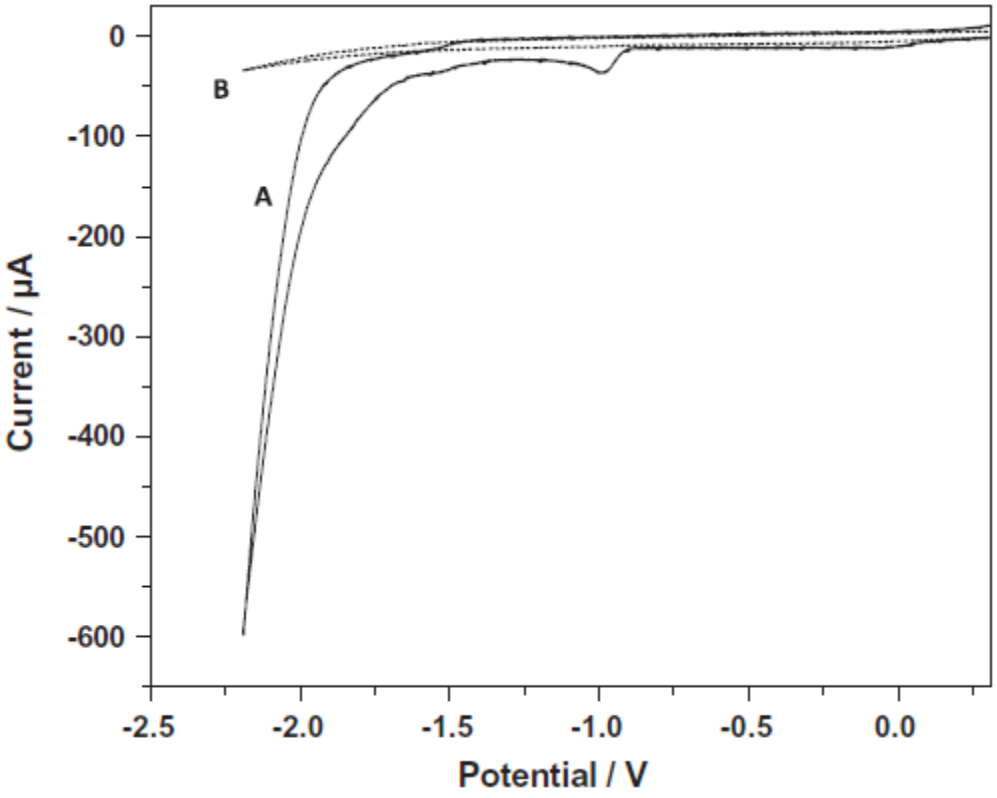

Figure (30). Cyclic voltammograms recorded with a glassy carbon disk electrode (area = 0.077 cm2) at 100 mV s^{-1} in oxygen-free CH_3CN- 0.050 M $TMABF_4$ containing (A) 5.0 mM 4-methyl-2-oxo-2H-chromen-7-yl acetate (2) or (B) 5.0 mM 4,40- (ethane-1,2-diyl)bis(2-oxo-2H-chromene-7,4-diyl) diacetate (3). Scans go from ca. + 0.25 to - 2.25 to + 0.25 V.

Electrochemical Study of 4-Hydroxy-3-nitrocoumarin

Cyclic voltammograms of 1 mM solution of 4-hydroxy-3-nitrocoumarin (**4**) in aqueous solutions at various pHs are shown in Figure 31. Over a pH range from 2.0 to 8.0, cyclic voltammograms show one cathodic (C_1) and anodic (A_1) peak which corresponds to the reduction of 4-hydroxy-3-nitrocoumarin (**4**) to 3-amino-4-hydroxycoumarin (**4a**) and oxidation of 3-amino-4-hydroxycoumarin (**4a**) to 4-hydroxy-3-(hydroxyamino)-coumarin (**4b**) (Scheme 2).

As Figure 31 shows, the peak potentials for peaks C_1, and A_1 shifted to the negative potentials by increasing pH. This is expected because of the participation of protons in the reduction of **4** to **4a** and oxidation of **4a** to **4b**. Controlled-potential coulometry was performed in aqueous solution containing 0.29 mmol of 4-hydroxy-3-nitrocoumarin (**3**) in a divided cell at -0.85 V (*vs.* SCE). Monitoring of the progress of the electrolysis was carried out by cyclic voltammetry (Figure 32). As shown, during coulometry, in parallel with the decrease in height of the cathodic peak C_1, the height of anodic peak A_1 increases. At the end of the coulometrycathodic peak C_1 disappears and only anodic peak A_1 remains. The cathodic peak C_1 disappears when the charge consumption becomes about $6e^-$ per molecule of **4** (Figure 32,inset). These voltammetric and coulometric data in addition to mass spectroscopic data (*m/z* = 177) of the final product in accompany with previous reports on chemical or electrochemical reduction of **4 [91-93]**confirm formation of 3-amino-4-hydroxycoumarin (**4a**) in electrochemical reduction of 4-hydroxy-3-nitrocoumarin (**4**) (Scheme 2, Eq. 1)**[94].**

Scheme (2)

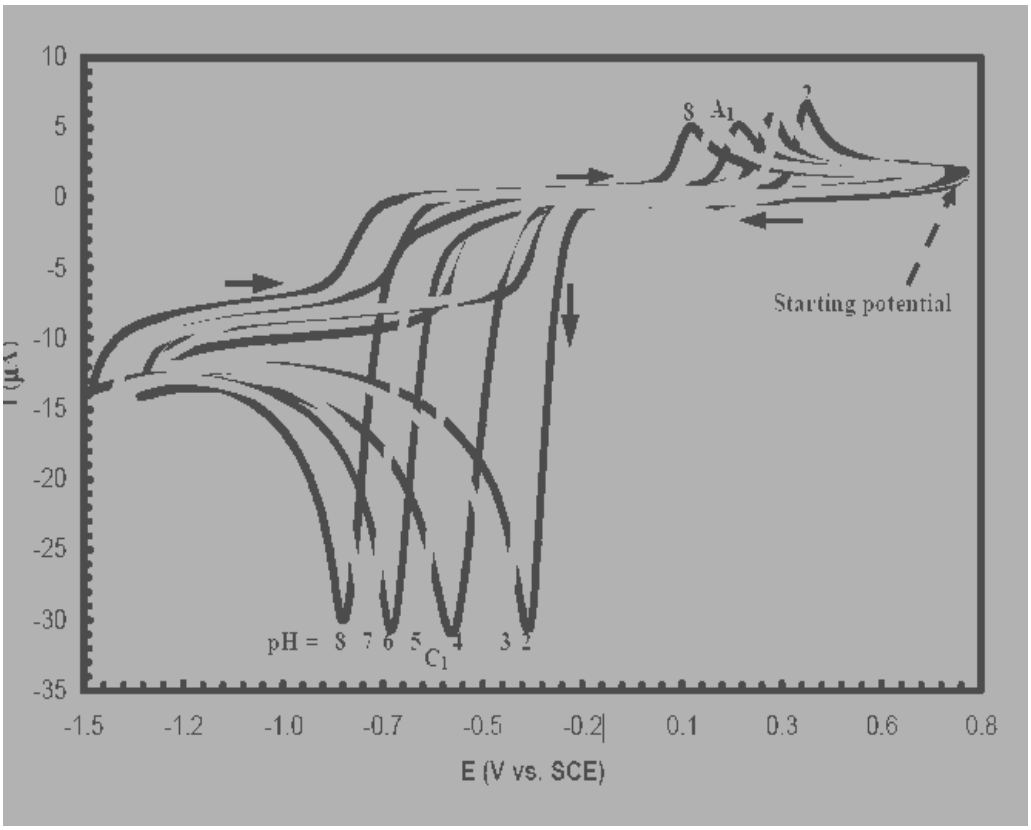

Figure (31).Cyclic voltammograms of 1 mM 4-hydroxy-3-nitrocoumarin at glassy carbon electrode (1.8 mm diameter), in various pHs (2.0, 3.0, 4.0, 5.0, 6.0, 7.0 and 8.0). Scan rate: 100 mV s-1; t = 25 °C.

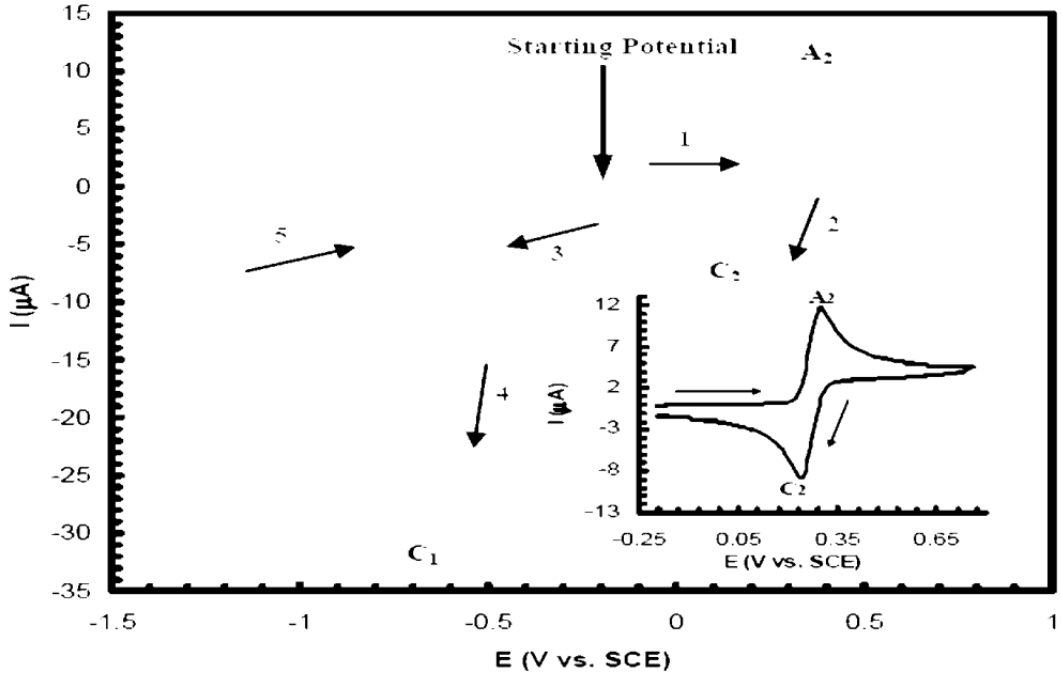

Figure (32).Cyclic voltammograms of 0.29 mmol 4-hydroxy-3-nitrocoumarin in phosphate buffer solution (*c* = 0.2 M, pH6.0), at glassy carbon electrode (1.8 mm diameter) during controlled-potential coulometry at -0.85 V *vs*. SCE. After consumption of: 0.0, 48.0, 96.0 and 144.0 C. Scan rate 100 mV s-1. t = 25 ± 1 °C. Inset: variation of peak current (*I*pC1) *vs*. charge consumed.

Electrochemical study of new 3-(hydroxyphenyl)benzo[f]coumarins

CVs of compounds 5, 6 and 7, that have the same number of hydroxylated substituents, were carried out in the pH range between 1.3 and 12.3, at different concentrations, and the results compared. CV in 20 µM of compound 5, in acetate buffer pH 5.3, showed an irreversible oxidation due to phenol oxidation. The oxidation of compound 5 gives rise to the formation of a reversible phenol oxidation product that corresponds to a catechol moiety, Due to the occupancy of compound 5 para position it is not possible the phenol oxidation to give rise to the formation of a hydroquinone. In the case of compounds 6 and 7, both ortho and para positions are unrestricted (in the case of compound 6, both ortho positions). Therefore, in acetate buffer pH 5.3, compounds 6 and 7 phenol oxidation process gives rise to two oxidation products, due to the formation of a catechol and a hydroquinone. Compound 6 irreversible phenol oxidation potential. The reversible phenol oxidation products, The strong adsorption of compound 6 phenol oxidation products at the surface of the GCE was demonstrated when, after several potential scans in the solution, the electrode was rinsed with a jet of deionized water and transferred to the supporting electrolyte, where the CV showed the reversible peaks, and the current remained constant in successive scans, In compound 7 the peak potentials were very similar to those of compound 6, and the two phenol oxidation product peaks are due to a catechol and hydroquinone moiety. Compound 7 irreversible phenol oxidation peak corresponds to one electron transfer. The reversible phenol oxidation product. Increasing the number of scans peaks. **[95]**

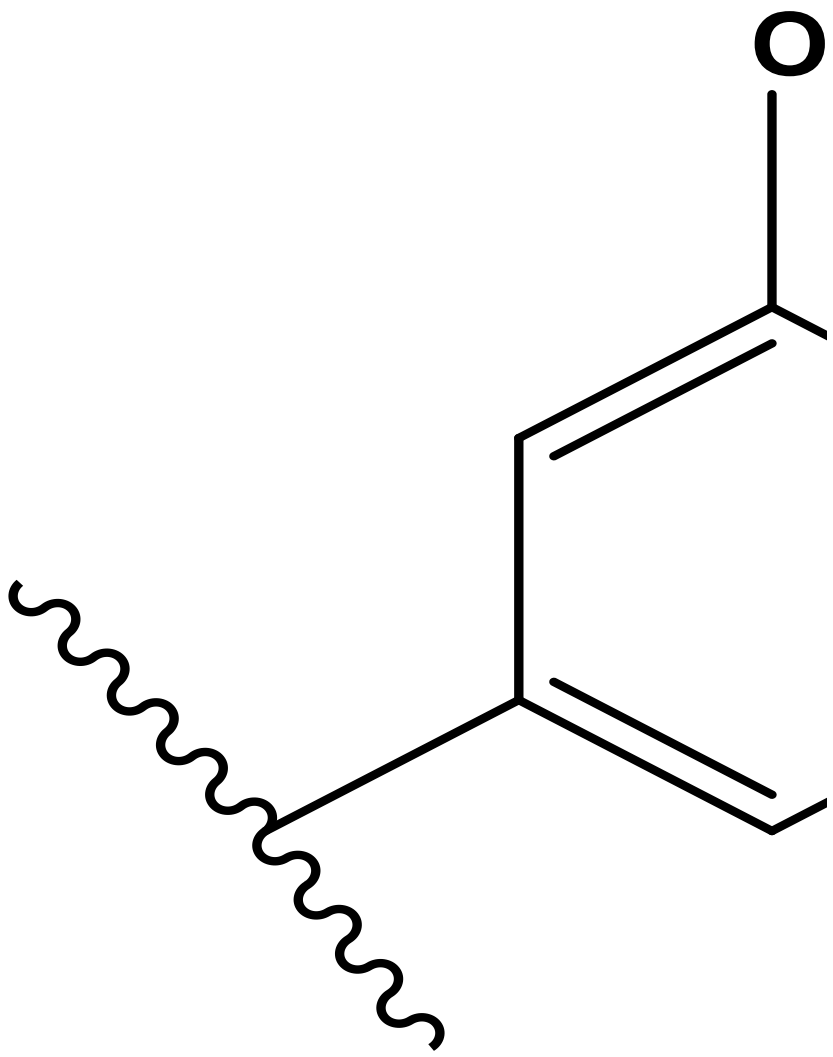

Compo

Reduction of Dihydropyridine-fused and pyridine-fused coumarins on a glassy carbon electrode in dimethylformamide

Coumarins (2H-benzopyran-2-ones) are a group of compounds that are present in many plants, fungi and bacteria with varied applications in traditional medicine. Interest in their chemistry arises from the diversity of their pharmacological activities, which are manifested particularly in hydroxylated derivatives **[96-98]**. Natural and synthetic coumarins possess anti-oxidant, antiinflammatory, anti-coagulation and anticancer activities **[99].**However, reports on the electrochemistry of substituted coumarins or fused-coumarins are rather

limited in the literature. Moreover, studies on the electrochemical reduction of the endocyclic carbonyl group are scarce because this process is highly dependent on the substituents present on the coumarin moiety. The nature of the heterocyclic moiety condensed with the coumarin base structure significantly affects the reduction mechanism of the endocyclic carbonyl group. Thus, in pyridine-fused compounds, CV reduction includes an EEC mechanism with dianion formation ($X\text{-}Py^{2-}$ in reaction (2) of the proposed mechanism).During electrolysis; the time-scale of the experiment drastically changes. Under these conditions, the $X\text{-}Py^{\cdot -}$ species can be protonated by any proton donor present in solution to generate the neutral radical $X\text{-}Py(H)^{\cdot}$, which is more easily reduced than the starting X-Py species, and the overall process involves reactions (1), (4) and (5).

$$X\text{-}Py + e^{-} = X\text{-}Py^{\cdot -} \qquad E_1 \qquad (1)$$

$$X\text{-}Py^{\cdot -} + e^{-} = X\text{-}Py^{2-} \qquad E_2 \qquad (2)$$

$$X\text{-}Py2^{-} + HA = X\text{-}Py\,(H)^{-} + A^{-} \qquad k_{p3} \qquad (3)$$

$$X\text{-}Py^{\cdot -} + HA = X\text{-}Py\,(H)^{\cdot} + A^{-} \qquad k_{p4} \qquad (4)$$

$$X\text{-}Py\,(H)^{\cdot} + e^{-} = X\text{-}Py(H)^{-} \qquad E_3 \qquad (5)$$

$$X\text{-}Py\,(H)^{-} + HA = X\text{-}Py\,(H)^{2} + A^{-} \qquad k_{p6} \qquad (6)$$

Conversely, the first reduction peak of the dihydropyridine fused coumarins follows an ECEC type mechanism with a father–son reaction to produce a hemiacetal derivative (Scheme 5). The second reduction peak is due to further reduction of the conjugate base formed from the father–son reaction (species III in Scheme 5). The electrochemical reduction mechanism was corroborated by ESR experiments. The theoretical study generated a spin density map of H-CPy radical species delocalised mainly within the coumarin moiety, indicating that the reduction of the endocyclic carbonyl group is occurring. The endocyclic carbonyl groups of pyridine-fused coumarins are easier to reduce than those of dihydropyridine-fused coumarins. The conjugation between the phenyl ring and the endocyclic carbonyl group significantly influences the reduction process of this group. **[100]**

Scheme (5).Proposed reduction mechanism for the endocyclic carbonyl group of coumarin[3,4-c]dihydropyridines in DMF.

Cathodic dimerization0f 7-methyl-2H-[1,4]dioxino[2,3-h]chromen-9(3H)-one.

Formation of the dimers can be explained with the fact that free radical anions ($R^{\bullet -}$) are produced as intermediate products after the uptake of one electron in the first step, i.e. in the cathodic direction. Since the radical anions formed are sufficiently basic, they underwent a rapid protonation ($RH^{\bullet}$) in the protic medium investigated indicating that the reaction sequence is successively $e^{-}+H^{+}$, i.e. EC, for the first step. The radicals ($RH^{\bullet}$) formed in the first step underwent cathodic dimerization by a chemical reaction, i.e. C in the second step, by the combination of like species yielding the corresponding stable dimers (RH–RH), i.e. ECC at the time of coupling. These findings are also consistent with similar studies concerning electrochemical reduction ofchalcone on mercury electrodes **[101]**.On the basis of CV, Coulometric and spectroscopic results the following general mechanism for the electrodimerization pathway of the compound 8 can be given as:

$$R + e^{-} \qquad R^{\bullet -} + H^{+} \text{ (rapid)} \qquad RH^{\bullet} \qquad (1)$$

$$2RH^{\bullet} \qquad RH\text{-}RH \qquad (2)$$

Therefore, Cathodic dimerization of the compound 8 was assigned to an ECC sequence **[102].** A more detailed possible electrodimerization mechanism proposed for 8 was also given in Scheme 6 below **[103].**

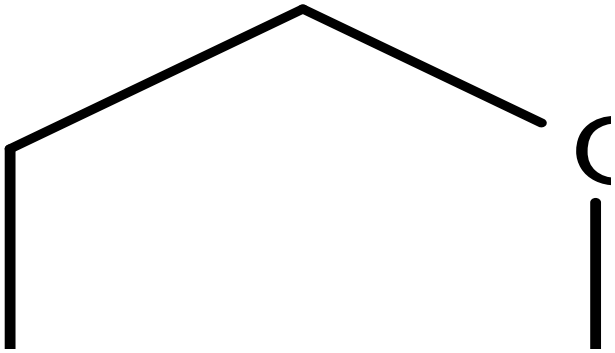

Scheme (6). A more detailed cathodic dimerization mechanism proposed for 8.

Electroreductive Dimerization of Coumarin and Coumarin Analogues at Carbon Cathodes

Electrochemical reduction of coumarin (10), 6-methylcoumarin (11), 7-methylcoumarin (12), 7-methoxycoumarin(13), and 5,7-dimethoxycoumarin (14) at carbon cathodesin dimethylformamide containing 0.10 M tetra-n-butylammoniumtetrafluoroborate has been investigated by means ofcyclic voltammetry and controlled-potential (bulk) electrolysis.Cyclic voltammograms for reduction of 10−14 exhibit twoirreversible cathodic peaks: (a) the first peak arises from oneelectronreduction of the coumarin to form a radical−anionintermediate, which is protonated by the medium to give aneutral radical; (b) although most of this radical undergoesself-coupling to yield a hydrodimer, reduction of the remainingradical (ultimately to produce a dihydrocoumarin) causes the second cathodic peak. At a potential corresponding to the firstvoltammetric peak, bulk electrolysis of 10−14 affords the corresponding hydrodimer as a mixture of meso and dl diastereomers.Although the meso form dominates, the dl-to-meso ratio varies, due to steric effects arising from substituents on the aromatic ring.Electroreduction of an equimolar mixture of 10 and 13 gives, along with the anticipated symmetrical hydrodimers, anunsymmetrical product derived from the two coumarins. A mechanistic

scheme involving both radical−anion and radicalintermediates is proposed to account for the formation of the various products.**[104]**

SCHEME (7) :Structures of Coumarins 10−14 and Coumarin-Derived Dimers D11, D22, D33, D44, D55, and D14

Antioxidant and Antiradical Properties of Some Examples of Flavonoids and Coumarins—Potentiometric Studies

According to results of cyclic voltammetry, it can be noted that the type of voltammogram directly depends on the relative position of hydroxyl groups in the molecule. The obtained voltammograms can be conditionally divided into three groups by type:

- The presence of an oxidation peak in the potential range of 0.21 to 0.28 V (Figure 1). Such compounds include luteolin, nordalbergin, 4-methylesculetin, 4-methyldaphnetin, and 7,8-dihydroxy-4-methyl-chroman-3-toluene-2-one. Compounds of this group contain in their structure a catechol fragment, which is characterized by reversible oxidation-reduction and an uncomplicated process of electron transfer from the antioxidant molecule.

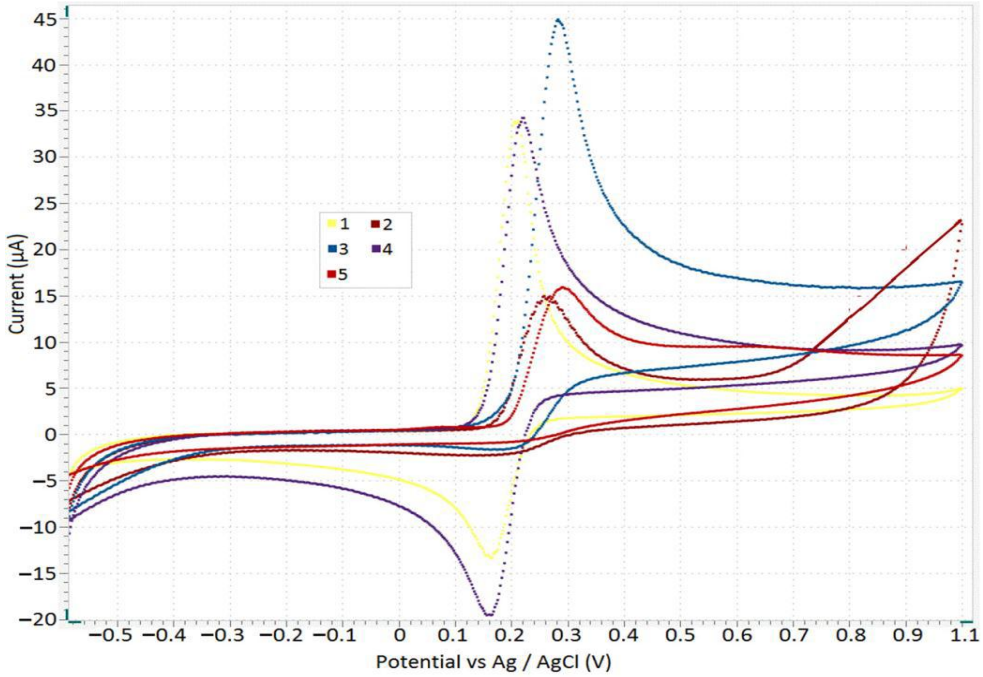

Figure 33. Cyclic voltammograms of 7,8-dihydroxy-4-methyl-chroman-3-toluene-2-one (1), Luteolin (2), 4-Methylesculetin (3), 4-Methyldaphnetin (4), and Nordalberginluteolin (5) recorded on a glassy carbon electrode, reference electrode—silver chloride electrode, C(AO) = 0.1 mM. Background:

phosphate buffer solution–ethanol 1:1. Scan rate is 0.05

- The presence of two peaks of oxidation: the position of the first peak is in the potential range of 0.08 to 0.11 V and the position of the second peak is in a more positive range of potentials. These compounds include quercetin, dihidromyricetin, and baicalein (Figure 2). The compounds contain a catechol/pyrogall fragment. The presence of two peaks may indicate a stepwise oxidation process. In this case, oxidation in the second stage can be difficult.

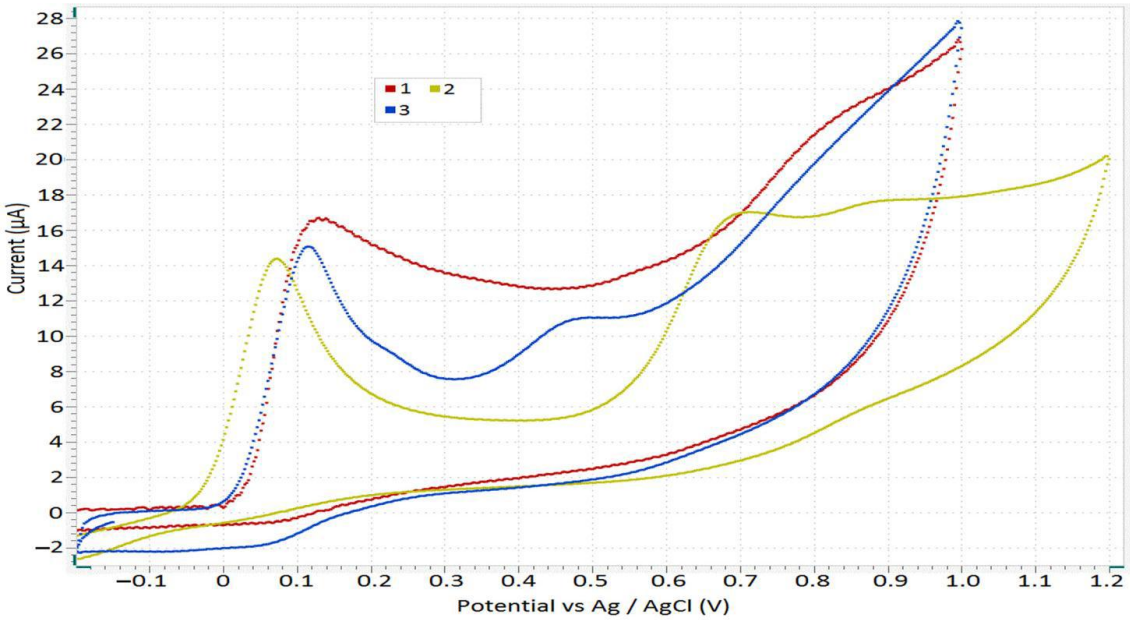

Figure 34. Cyclic voltammograms of Dihidromyricetin (1), Baicalein (2), and Quercetin (3) recorded on a glassy carbon electrode, reference electrode—silver chloride electrode, CAO = 0.1 mM. Background: phosphate buffer solution–ethanol 1:1. Scan rate is 0.05 V/s.

Scheme (8)**.** Quercetin oxidation reaction.

- The last group is characterized by the presence of an oxidation peak in a rather positive potential range (0.50 to 0.80 V) (Figure 3). These compounds include silybin,

chrysin, genistein, apigenin, and 4-methyl-5,7-dihydroxycoumarin. The compounds of this group contain a resorcinol fragment, which is characterized by hindered electron transfer from functional OH groups of molecules and, as a rule, lack of antioxidant action by the electron transfer mechanism. [105].

References

[1]. D. K. Gosser, Cyclic Voltammetry, VCH publishers, Inc., New York (1994).
[2]. J. Koryta, J. Dvorak, Principles of Electrochemistrey, 1st ed. John Wiley and sons; New York (1987).
[3]. G. J. Hills in " Reference electrodes: Theory and practice (D. J. G. Lves and G. J. Janzeds.)" Academic press, New York (1961).
[4]. J. W. Butter, advan. J. W. Butter, advan. Electrochem. chemotrochem. Eng. 7, 77 (1970).
[5]. A. N. Dey and E. J. Rudd, Electrochem. Soc. Meet., spring p. 463 (1973).
[6]. H. Lund. And P. Lversen" Inorganic Electrochemistry" (M. M. Baizer, ed.) chapter IV p. 165 Dekker New York (1973).
[7]. C. K. Mann. Electroanal. Chem. 3, 57 (1969).
[8]. S. Andreades and E. W. Zahnow, J. Amer. Chem. Soc. 91, 4181 (1969).
[9]. J. P. Billon, J. Electronal. Chem. 1, 486 (1960).
[10]. R. EviscoElectrochem. Soc. Meet., Spring p. 67 (1967).
[11]. M. Breant, M. Bazion, C. Buisson, M. Dupin, and J. M. Rebattu, Bull. Soc. Chim. Fr. p. 5065 (1968).
[12]. J. A. Riddick and W. B. Bunger, Tech. Chem. 2, 552, and 572 (1970).
[13]. G. J. Janz and R. P. T. Tomkins "Nonaqueous Electrolytes Hand Book", Vol. 1, Academic press, New York. (1972).
[14]. Ross Finkelstein Rudd Academic press New York San Francisco London (1975).
[15]. E. J. Rudd, M. Finkelstein and S. D. Ross, J. Org. Chem. 37. 1763 (1972).
[16]. Y. V. Pleskov, Y. Y. Gurevich. Semiconductor Photoelectrochemistry. Consultants Bureau: New York (1986).
[17]. L. I. Antropov, Theoretical Electrochemistry. Mir: Moscow (1972).
[18]. J. Goodisman, Electrochemistry: Theoretical Foundation, 1st ed. John Wiley and sons. New York (1987).
[19]. P. Kebarle, S. Chowdhury, Chem. Rev. 87, 514 (1987).
[20]. J. H. Hupp, M. J. Weaver, Inorg. Chem. 23, 3639 (1984).
[21]. J. K. Kochi, Angew. Chem. Int. Ed. Engl. 27, 1227 (1988).
[22]. J. M. Saveant, Single Elestron Transfer and Nucleophilie Substitution. Advances in Organic Chemistry, Vol. 26. Academic press: London (1990).
[23]. R. D. Allendorfer, P. H. Rieger, J. Am. Chem. Soc. 87, 2336 (1965).
[24]. A. J. Fry, W. E. Britton, Eds. Topics in Organic Electrochemistry, 1st ed. Plenum press. New York (1986).
[25]. K. Y. Lee, D. J. Kuchynka, J. K. Kochi, Inorg. Chem. 29, 4196 (1990).
[26]. H. Kojima, A. J. Bard, J. Am. Chem. Soc. 97, 6317 (1975).
[27]. R. A. Marcus, J. Phys. Chem. 94, 1050 (1990).

[28]. R. A. Marcus, ibid, 94, 4152 (1990).
[29]. R. A. Marcus, ibid, 95, 2010 (1991).
[30]. J. M. Saveantet. Al., Chem. Rev. 3, 92 (1992).
[31]. D. K. Gosser. Jr., P. H. Rieger, Anal. Chem. 60, 1159 (1988).
[32]. A. C. Testa and W. H. Reinmuth, Anal. Chem. 33, 1320 (1961).
[33]. R. S. Nicholson, and I. Shain, Anal. Chem. 36, 706 (1964).
[34]. S. W. Feldberg, J. Electroanal. Chem. 49, 290 (1990).
[35]. D. Briz, Digital Simulation in Electrochemistry, 2nd ed. Springer Verlag: Berlin (1988).
[36]. C. P. Andcieux, P. Hapiot, J. M. Saveant, Chem. Rev. 90, 723 (1990).
[37]. Y. Zhang, D. K. Gosser, Jr., P. H. Rieger, D. A. Swiegart, J. Am. Chem. Soc. 113, 4062 (1991).
[38]. A. J. Bard, L. R. Faulkner, Electrochemical Methods, 1st ed. John. Wiley and sons: New York (1980).
[39]. F. Zhang, D. K. Gosser. Jr., S. R. Meshnick, Bio. Pharm. (1992).
[40]. S. R. Meshnick, A. Thomas, A. Ranz, Xu. C. M; pan, H. Z. Mol. Biochem. Prasitol. 49, 181 (1991).
[41]. K. Aoki, J. Osteryoung, J. Electroanal. Chem. 19, 122 (1981).
[42]. P. T. Kissenger, In Laboratory techniques in Electroanalytical Chemistry, 1st ed. P. T. Kissenger, W. R. H ineman, Eds. Marcel Dekker New Yoork Chapter 22 (1984).
[43]. W. J. Bowyer E. E. Engeiman, D. H. Evans. J. Electroanal. Chem. 67, 262 (1989).
[44]. D. K. Gosser. Jr., F. Zhang, Talanta 38, 715 (1991).
[45]. K. Y. Lee, C. Amatore, J. K. Kochi, J. P hys. Chem. 95, 1285 (1991).
[46]. W. M. Schwartz, I. Shahin, J. Phys. Chem. 69, 30 (1965).
[47]. V. Parker, W. E. Britton, and A. J. Fry, Eds. Topics in Organic Electrochemistry, 1st ed. Plenum Press: New York (1986).
[48]. R. J. Klinger, J. K. Kochi, J. Phys. Chem. 86, 1731 (1981).
[49]. Q. Huang, D. K. Gosser, Jr., Talanta 39 (9), 1155 (1992).
[50]. D. Lexa, J. M. Saveant, J. Am. Chem. Soc. 100, 3220 (1978).
[51]. P. He, L. R. Faulkner, Anal. Chem. 58, 517 (1976).
[52]. Yu. V. Pleskov and V. Yu. Filinovskii New York and London (1976).
[53]. P. H. Rieger, Electrochemistry. Prentice-Hall Engel-Wood Cliffs, NJ. (1987).
[54]. R. Greff; R. Peat;; L. M. Peter, D. Pletcher, J. Robinson, Instrumental Methods in Electrochemistry. Ellis Horwood: Chichester (1985).
[55]. C. P. Andrieux; P. Hapiot, H. M. Saveant, Chem. Rev. 90, 723 (1990)
[56]. Brace, L. A., J. Medical Technology, 49, 457, (1983).
[57]. Lake, B. G., Archieves of Toxicology, 7, 16, (1984).
[58]. Yuen, S. H., Analyst, 103, 842, (1978).
[59]. Raw, G. R., Colaborative International Pesticides Analytical Council (CIPAC); Heffer, W. & Sons Ltd: Cambridge, U.K., 1, 696, (1970).
[60]. Salaman, M. H., J. Cancer, 9, 177, (1967).
[61]. Hogan, E. C., Fed. Cosmet. Toxicol., 5, 141, (1967).
[62]. Zhang, F. G. and Yu, C. L., J. Appl. Phys., 62, 49, (1987).
[63]. Jones, G. II and Rahman, M. A., J. Phys. Chem., 98, 13028, (1994).
[64]. Nemkovich, N. A.; Reis, H.; Baumann, W., J. of Luminescence, 71, 255, (1997).
[65]. Gautier-Thianche, E.; Sentein, C.; Nunzi, J. M.; Lorin, A.; Denis, C. and Raimond, P., Synthetic Metals, 91, 323, (1997).
[66]. Justin Thomas, K. R.; Lin, J. T.; Tao, Y. T. and Ko, C. W., J. Am. Chem. Soc., 123, 9404, (2001).
[67]. Chen, C. H. and Tang, C. W., Applied Physics Letters, 79, 3711, (2001).
[68]. Kang, S. C.; Oh, S. I. and Kim, K., J. Bull. Korean Chem. Soc., 11(6), 505, (1990).
[69]. Huang, Y.; Lu, Z. Y.; Peng, Q.; Xie, R. G.; Xie, M. G.; Peng, J. B. and Cao, Y., J. of Materials Science, 40, 601, (2005).
[70]. Mal, N. K.; Fugiwara, M.; Tanaka, Y., Nature, 421, 350, (2003).
[71]. Wang, Z. S., J. Phys. Chem., B, 109, 3907, (2005).
[72]. Harle, A. J. and Lyons, L. E., J. Chem. Soc., 1575, (1950).
[73]. Capka, O. and Czech. C., Chem. Commun., 15, 965, (1950).
[74]. Zuman, P., Chem. Listy, 48, 94, (1954).
[75]. Zuman, P., Organic Polarographic Analysis; Pergamon Press: New York 251, (1964).
[76]. Zuman, P., Substituent Effects in Organic Polarography; Plenum Press: New York 165, (1967).
[77]. Gourley, R. N.; Grimshaw, J. and Miller, P. G., J. Chem. Soc. (C), 2318, (1970).
[78]. Reddy, B. O.; Reddy, A. V.; Raju, K. M.; Rao, A. K., J. Electrochem. Soc. India, 35, 319, (1989).
[79]. Partridge, L. K.; Tansley, A. C. and Porter, A. S., Electrochemical Acta, 11517, (1966).
[80]. Bond, A. M. and Thomas, F. G., Langmuir, 4, 341, (1988).
[81]. Helin, M.; Jiang, Q.; Ketamo, H.; Hakansson, M.; Spehar, A. M.; Kulmala, S. and Ala-Kleme, T., Electrochimica. Acta., 51, 725, (2005).
[82]. Carrazon, J. M. P.; Vergara, A. G.; Garcia, A. J. R. and Diez, L. M. P., Anal. Chim. Acta, 216, 231, (1989).
[83]. Dempsey, E.; O'Sullivan, C.; Smyth, M. R.; Egan, D.; O'kennedy, R. and Wang, J., J. Pharm. Biomed. Anal., 11, 443, (1993).
[84]. Dempsey, E.; O'Sullivan, C.; Smyth, M. R.; Egan, D.; O'kennedy, R. and Wang, J., Analyst, 118, 411, (1993).
[85]. Wu, Q. and Dewald, H. D., Electroanalysis, 13, 45, (2001).
[86]. Wang, Z. S., J. Phys. Chem., B, 109, 3907, (2005).
[87]. Zuman, P., Substituent Effects in Organic Polarography; Plenum Press: New York 165, (1967).
[88]. Zuman, P., the Elucidation of Organic Electrode Processess; Acdemic Press: New York, 7, (1969).
[89]. Kim, S. H.; Jung E. J.; So, E. M.; Shen, C. Z.; Chun, H. J.; Kim, Y. M. and Kim, I. K., Bull. Korean Chem. Soc., 27, 9, (2006).
[90]. Rheinhardt, J. H.; Mubarak, M. S.; Foley, M. P. and Peters, D. G., J. Electroanalytical Chemistry, 654, 44–51, (2011).
[91]. Heubner, C.F. and Link, R. P., J. Am. Chem. Soc., 67, 99, (1945).
[92]. Trkovnik, M.; Laan M.; Stuni, Z. and Nahmijaz, D., Org. Prep. Proced. Int., 7, 47, (1975).
[93]. Radanyi, C.; Bras, G. L.; Messaoudi, S.; Bouclier, C.; Peyrat, J. F.; Brion, J. D.; Marsaud, V.; Renoir, J. M. and Alami, M., Bioorg. Med. Chem. Lett., 18, 2495, (2008).
[94]. Nematollahi D. and Karbasi H., J. Iran. Chem. Soc., 8, 1, 48-58, (2011).
[95]. Matos, M. J.; Janeiro, P.; Santana, L.; Uriarte E. and Oliveira-Brett, A. M., J. of Electroanalytical Chem., 726, 62–70, (2014).

[96]. Fylaktakidou, K. C.; Hadjipavlou-Litina, D. J.; Litinas, K. E. and Nicolaides, D. N., Current Pharmaceutical Design, 10, 3813, (2004).
[97]. Voora, D.; McLeod, H.L.; Eby, C. and Gage, B.F., Pharmacogenomics 6, 503, (2005).
[98]. Lin, H.C.; Tsai, S.H.; Chen, C.S.; Chang, Y.C.; Lee, C.M.; Lai, Z.Y. and Lim, C.M., Biochemical Pharmacology, 75, 1416, (2008).
[99]. Lin, W.L.; Wang, C.J.; Tsai, Y.Y.; Liu, C.L.; Hwang, J.M. and Tseng, T.H., Archives of Toxicology, 74, 467, (2000).
[100]. Nu˜nez-Vergara L. J.; Pardo-Jiménez, V.; Barrientos, C.; Olea-Azar, C. A.; Navarrete-Encina, P. A. and Squella, J. A., ElectrochimicaActa, 85, 336– 344, (2012).
[101]. Tavares, E. M.; Carvalho, A. M.; Gonçalves, L. M.; Valente, I. M.; Moreira, M. M.; Guido L. F.; Rodrigues, J. A.; Doneux, T. and Barros, A. A., Electrochem. Acta., 90, 440–444, (2013).
[102]. Bard, A. J. and Faulkner, L. R., Electrochemical Methods, 1st ed. John. Wiley and sons: New York (1980).
[103]. Tuğral, S. and Berkem, M. L., Journal of Molecular Liquids, 196, 363–369, (2014).
[104]. Pasciak, E. M.;Rittichier, J. T.;Chen, C.; Mubarak, M. S.;VanNieuwenhze, M. S. and Peters, D. G., J. Org. Chem., 80, 274−280, (2015)
[105]. Gerasimova E. ;Gazizullina E. ; Radosteva E. and Ivanova A., Chemosensors, 9, 112, (2021) .